metals

MDPI

Article

Novel Method of Bauxite Treatment Using Electroreductive Bayer Process

Andrei Shoppert [1,2,*], Dmitry Valeev [3] and Irina Loginova [2]

[1] Laboratory of Advanced Technologies in Non-Ferrous and Ferrous Metals Raw Materials Processing, Ural Federal University, 620002 Yekaterinburg, Russia
[2] Department of Non-Ferrous Metals Metallurgy, Ural Federal University, 620002 Yekaterinburg, Russia; i.v.loginova@urfu.ru
[3] Laboratory of Sorption Methods, Vernadsky Institute of Geochemistry and Analytical Chemistry of the Russian Academy of Sciences, 119991 Moscow, Russia; dmvaleev@yandex.ru
* Correspondence: a.a.shoppert@urfu.ru

Abstract: Reductive leaching in the Bayer cycle using iron (2+) allows for Al extraction to be significantly increased through the magnetization of Al-goethite and Al-hematite. However, the use of expensive iron (2+) salts or iron powder as a source of iron (2+) leads to a significant increase in production costs. In this work, the feasibility of a new method, the reductive leaching of bauxite using an electrolysis process, was investigated. The reduction of iron minerals of boehmitic bauxite in both the Bayer solution and purely alkaline solutions was carried out. Experiments were performed using a plate cathode and a bauxite suspension in an alkaline solution, as well as using a bulk cathode with a stainless-steel mesh at the bottom of a cell as the current supply. During the electrolysis process, the potential of the cathode relative to the reference electrode was measured as a function of the current at different concentrations of solid (100–300 g L^{-1}) and suspension temperatures (95–120 °C). It was shown that the current efficiency using the suspension and plate cathode with the predominant deposition of Fe did not exceed 50% even with the addition of magnetite to increase the contact of the solid phase with the current supply. With the use of a bulk cathode, the reduction of iron minerals led predominantly to the formation of magnetite with the efficiency of using the electric current at more than 80%. As a result of the preliminary desilication and electroreduction, it was possible to extract more than 98% of Al from bauxite and to increase the iron content in the bauxite residue to 57–58%.

Keywords: hematite electroreduction; boehmitic bauxite; Al extraction; reductive leaching; red mud; bauxite residue; magnetite; waste utilization

check for updates

Citation: Shoppert, A.; Valeev, D.; Loginova, I. Novel Method of Bauxite Treatment Using Electroreductive Bayer Process. *Metals* **2023**, *13*, 1502. https://doi.org/10.3390/met13091502

Academic Editor: Denise Crocce Romano Espinosa

Received: 19 July 2023
Revised: 10 August 2023
Accepted: 15 August 2023
Published: 22 August 2023

Copyright: © 2023 by the authors. Licensee MDPI, Basel, Switzerland. This article is an open access article distributed under the terms and conditions of the Creative Commons Attribution (CC BY) license (https://creativecommons.org/licenses/by/4.0/).

1. Introduction

The Bayer process is used worldwide for the alumina production. This process involves the alkaline leaching of bauxite to extract Al, followed by the precipitation of $Al(OH)_3$ to recycle the solution [1–3]. The leaching process results in the formation of a solid residue, commonly referred to as a bauxite residue, which consists of iron minerals, hydrous aluminosilicates, which are formed through the interaction of aluminium and silicon compounds in a solution, and other impurity minerals [4–6]. Some of the aluminium in bauxite is present in the form of refractory at standard leaching alumogoethite (Al-goethite) and alumohematite (Al-hematite) [7–9]. The study of Li et al. [10,11] showed that reductive leaching can increase the Al extraction through the magnetization of Al-goethite and Al-hematite. The addition of iron (2+) can also decrease aluminium losses by preventing the formation of desilication products and sodium titanate [12]. Previously, iron (2+) sulphate ($FeSO_4$) [13], organic compounds [14] and iron powder [15] were suggested for the magnetization of iron minerals. However, the use of additional reagents increases the cost of the alumina production process; therefore, in this work, the possibility of using electrolysis for iron mineral reduction was investigated.

Hematite (Fe_2O_3) is the most studied raw material for the electroreduction of metallic iron. Studies have been carried out both in suspensions [16–18] and in bulk ceramic cathodes [19–21]. Despite the low electrical conductivity, electrodeposition and electroreduction of Fe_2O_3, it was found that this process was feasible. Current yields in excess of 90% have been obtained using NaOH solutions with concentrations in excess of 50% [22]. Various raw materials are being considered for electrochemical reduction to produce metallic iron, including iron-rich wastes such as BR from the aluminium industry [23,24].

Maihatchi et al. [23] investigated the possibility of the electrochemical reduction of hematite ore and iron minerals in BR (Alteo, France). It was shown that the use of BR and highly concentrated solutions of caustic alkali (500 g L^{-1} NaOH) at 110 °C led to a significant decrease in current yield compared to hematite ore. The greatest difference was observed at a high current density (above 100 A m^{-2}, where the current yield for hematite was more than 80% and for BR did not exceed 30%). According to the authors, the decrease in electrolysis efficiency when using BR was due to the large number of impurities in the BR, which prevented the adsorption of hematite on the cathode surface. This was confirmed through the addition of commercial hematite and aluminosilicates at different ratios.

Koutsoupa et al. [24] researched the possibility of hematite reduction from BR in a highly concentrated alkaline solution (50% NaOH or 762,7 g L^{-1} NaOH). The results showed that the Faradaic current efficiency was strongly dependent on the process temperature. The highest current efficiency (>70%) was obtained at a temperature of 125 °C, and a decrease in temperature or an increase in temperature led to a significant decrease in current efficiency to 30–40%. This phenomenon is due to the insufficient rate of iron dissolution at low temperatures and the presence of a significant number of gas bubbles in the solution near the boiling point, which prevents contact with the cathode.

The mechanism of the electrochemical reduction of hematite can be described by the following chemical reactions. A strong solution of caustic alkali can dissolve hematite and turn it into sodium ferrite. In water, some of the ferrite goes into the solution as hydroxocomplexes (Equation (1)) or precipitate in the form of iron hydroxide (Equation (2)).

$$Fe_2O_3 + 2NaOH = 2NaFeO_2 + H_2O, \quad (1)$$

$$FeO_2^- + 2H_2O = Fe(OH)_4^-. \quad (2)$$

The hydroxocomplexes are electrochemically reduced to $Fe(OH)_3^-$ (Equation (3)) or to iron (Equation (4)). $Fe(OH)_3^-$ can also interact with hematite to form magnetite (Equation (5)).

$$Fe(OH)_4^- + e^- = Fe(OH)_3^- + OH^-, \quad (3)$$

$$Fe(OH)_3^- + 2e^- = Fe + 3OH^-, \quad (4)$$

$$Fe_2O_3 + Fe(OH)_3^- = Fe_3O_4 + 4H_2O. \quad (5)$$

Hematite can be reduced using the solid-phase reaction to elemental iron (Equation (6)) and magnetite (Equation (7)). Under alkaline conditions, oxygen is converted into a hydroxyl ion, according to Equation (8):

$$Fe_2O_3 + 6e^- = 2Fe + 3O^{2-}, \quad (6)$$

$$3Fe_2O_3 + 2e^- = 2Fe_3O_4 + O^{2-}, \quad (7)$$

$$O^{2-} + H_2O = 2OH^-. \quad (8)$$

The magnetite formed through the reduction of hematite can also be reduced to iron (Equation (9)) and dissolved to form hydroxocomplexes (Equation (10)):

$$Fe_3O_4 + 8e^- = 3Fe + 4O^{2-}, \quad (9)$$

$$Fe_3O_4 + 4H_2O + OH^- + 2e^- = 3Fe(OH)_3{}^-. \quad (10)$$

According to the described system of equations, the process can proceed both in the solid phase (Equation (6)) or through the dissolution of hematite in an alkaline solution with a subsequent reduction to metallic iron (Equations (2)–(4)). The solubility of hematite in the alkaline solution is low, so when iron is released from the solution during electrolysis, this allows new amounts of hematite to dissolve (Equation (2)). Additionally, according to Equations (5) and (7), the reduction of hematite to magnetite is possible. It was shown in [18,25,26] that the current efficiency of magnetite electroreduction is the lowest in the hematite–oethite–magnetite sequence. Accordingly, magnetite formed using Equation (5) led to a decrease in the process efficiency. Under certain overvoltage conditions, a side reaction can also be presented due to the release of hydrogen. Hydrogen in turn can also reduce hematite. When the process is carried out at atmospheric pressure, the contribution of this reaction can be very low, as it is not possible to create the necessary concentration of hydrogen in the solution.

This study investigates the electrochemical reduction of iron minerals from bauxite suspended in an aluminate solution, which can be produced simultaneously with the Bayer leaching process. This would eliminate the need for additives in the Bayer reduction process. For this purpose, experiments were carried out on the reduction of iron minerals of high-iron boehmitic bauxite suspended in an alkaline solution. Experiments were carried out using a bauxite-based suspension and a plate cathode, as well as a bulk cathode. For the bulk cathode experiments, the slurry was thickened prior to electrolysis and the current flow was conducted through a stainless-steel mesh at the bottom of the cell. The solid phase obtained through electroreduction was then subjected to standard Bayer leaching to extract Al and complete the reduction of iron minerals. The solid phase obtained through the electrolysis of the suspensions and after high-pressure leaching was subjected to various physical and chemical analyses to determine the efficiency and the mechanism of the processes.

2. Materials and Methods

2.1. Materials

Bauxite from the Middle Timan deposit (Ukhta, Russia) was used as the raw material. The chemical and phase composition are presented in Table 1 and Figure 1, respectively. This bauxite type is characterized as having a high iron and silicon content. It requires high-pressure leaching in order to obtain an oversaturated aluminate solution. Our previous research [27] using Mössbauer spectroscopy showed that the bauxite contained high amounts of Al-goethite, Al-hematite and chamosite that were refractory for standard Bayer leaching.

Bauxite was premilled to obtain a class −73 μm of more than 80%, less than 100 μm—98%. To obtain a suspension, the crushed bauxite was mixed with a synthetic Bayer solution (150 g L^{-1} Al_2O_3 and 300 g L^{-1} Na_2O) or NaOH solution with a concentration of 400 g L^{-1} Na_2O to obtain the concentration of the solid in suspensions of 100, 200 and 300 g L^{-1}.

Table 1. Elemental composition of the raw bauxite, wt. %.

Al	Fe	Si	Ti	Ca	Mn	Mg	K	Na	O	μSi
27.64	18.03	3.02	1.60	0.60	0.41	0.28	0.17	0.05	47.51	8.07

μSi—the silica ratio of bauxite (the mass ratio of Al_2O_3 to SiO_2).

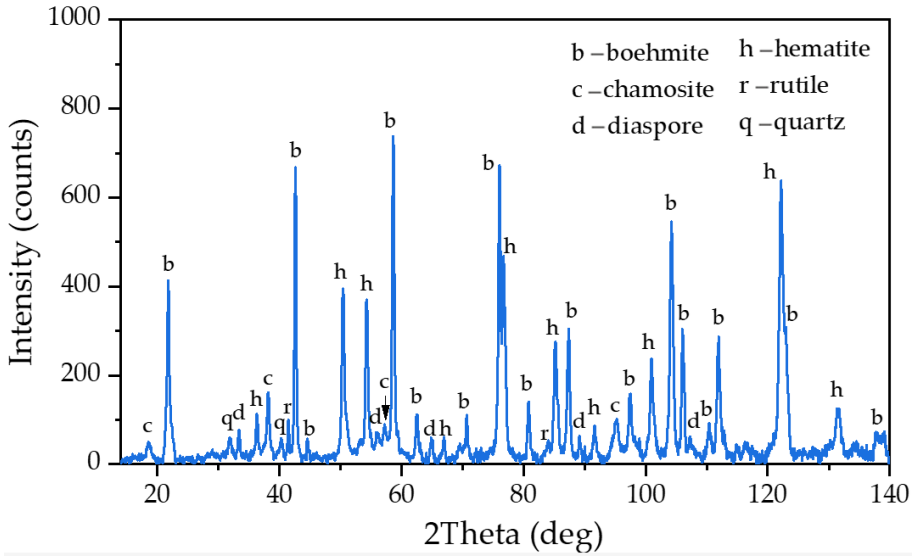


Figure 1. XRD pattern of raw bauxite from the Middle Timan deposit.

The solutions were obtained by mixing NaOH and $Al(OH)_3$ (if necessary) of analytical grade with distilled water and then stirring at 108 °C for 30 min. After leaching, the solutions were filtered with a Buechner funnel to separate the undissolved residue. In some experiments, magnetite concentrate was added in addition to the bauxite, the elemental and phase composition of which is shown in Table 2 and Figure 2, respectively. This concentrate was obtained through the reductive leaching of BR sands from the Friguia refinery (Guinea) in the presence of iron (2+) hydroxide, according to the method described in [28].

Table 2. The elemental composition of the magnetite concentrate obtained after reductive leaching of the Friguia alumina refinery bauxite residue (BR), wt. %.

Fe	Si	Ti	Al	Na	O	Other
69.55	0.34	1.01	0.15	0.24	27.81	0.90

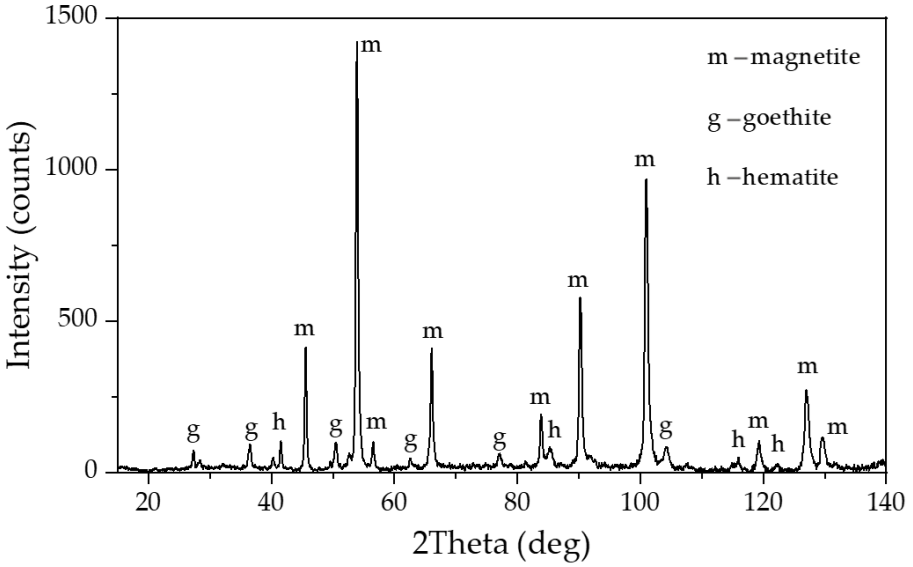


Figure 2. XRD pattern of magnetite concentrate obtained through leaching of bauxite residue (BR) from the Friguia plant in the presence of (2+) at T = 120 °C, τ = 120 min and C_{Na2O} = 330 g L^{-1}.

2.2. Experimental Setup

The schematic view of the experimental setup for the study of bauxite iron mineral reduction using electrolysis is shown in Figure 3.

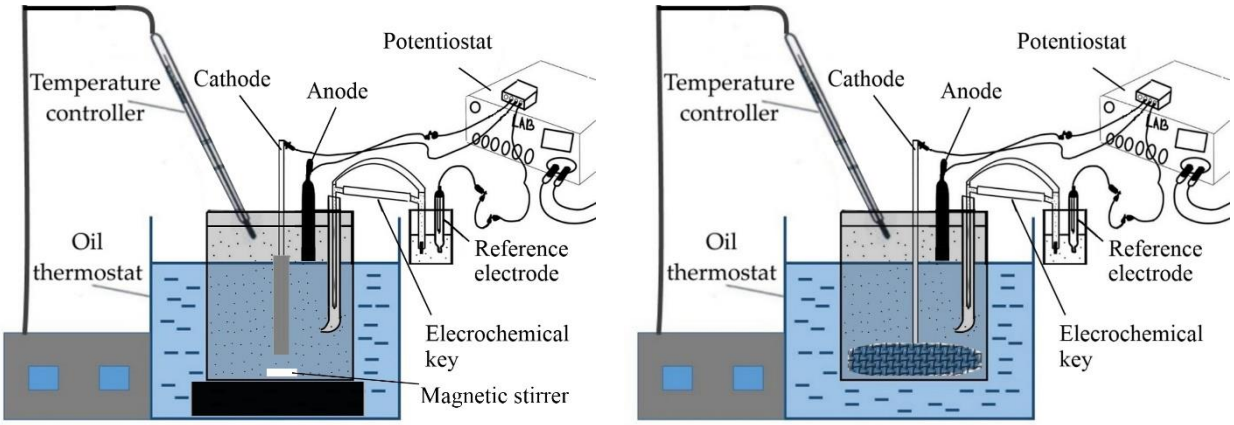


Figure 3. Schematic view of experimental setups used to study the process of electroreduction of bauxite iron minerals in alkaline media: (**a**) for experiments in suspension with a plate cathode with constant stirring; (**b**) for experiments with a bulk cathode (mesh current supply).

As shown in Figure 3a, the experimental setup consisted of a 500 mL glass beaker placed in an oil bath (DF-101S, Zhejiang Lichen Instrument Technology Co., Ltd., Shaoxing, China) equipped with a magnetic stirrer. The suspension was heated to the desired temperature inside the beaker before electrolysis. The temperature of the suspension was controlled using a temperature sensor, which was connected to the PID regulator of the oil bath. A stainless-steel plate cathode with an immersed area of 9.91 cm^2 was used as a current supply in the experiments with constant stirring of the suspension. During electrolysis, the potential of the cathode was measured relative to the reference electrode as a function of the current at different concentrations of solid (100–300 g L^{-1}) and suspension temperature (95–120 °C) using a ZiveLab SP 2 potentiostat (Zivelab, Seoul, Korea).

When using a bulk cathode, round pieces of mesh with diameters of 6 cm, 7 cm and 9.2 cm were used as the current supply. The area of the mesh, taking into account the dimensions of the mesh cells, the wire thickness and the length and thickness of the wire connecting the terminal of the potentiostat to the mesh, was 40 cm^2, 75 cm^2, and 110 cm^2, respectively. For the experiments with the bulk cathode, a 100 g bauxite sample was leached for 1 h with constant stirring using an overhead stirrer at a temperature of 120 °C in 1 L of an alkaline solution with a concentration of 400 g L^{-1} Na_2O in a stainless-steel reactor coated with PTFE with a volume of 2 L in order to preliminarily desilicate the bauxite. According to previous research, this step [27] helps increase the efficiency of the subsequent reductive leaching.

The resulting pulp was then subjected to thickening for a duration of 30 min. The underflow, containing 300 mL of sand, was separated from the clarified solution after 30 min of thickening, and the underflow was used for the potentiodynamic measurements and the electrolysis process at a constant current strength of 1.945 A and a pulp temperature of 120 °C. After electrolysis, the suspension was filtered using the Buchner funnel. The filtered and washed residue was then subjected to complete Al extraction using high-pressure Bayer leaching at 250 °C for 30 min in a steel bomb placed in the thermostat. After filtration and washing, the residues were dried at 110 °C for 8 h and then subjected to the analysis. A 10 cm^2 nickel plate was used as an anode. The reference electrode was a mercury–mercury-oxide electrode OH-/HgO, Hg (RE-1A, YM, Shaanxi, China). The potential of the electrode relative to the hydrogen electrode at 25 °C in 10 N KOH solution was 0.098 V. All potentials in the paper were given relative to the reference electrode. The

reference electrode was placed in a separate beaker connected to the main beaker using an electrochemical key (with Luggin capillary inside suspension) on a tripod outside the oil bath. The electrochemical key and the beaker with the reference electrode were filled with 10 N NaOH solution. The electrodes were connected to the corresponding terminals of the potentiostat.

2.3. Analysis

The mineralogy of the raw bauxite and the solid residue after alkaline leaching was measured with X-ray diffraction (XRD) using a Difrei-401 X-ray diffractometer (JSC Scientific Instruments, Saint Petersburg, Russia) with a Cr-Kα radiation source and a 2θ range of 14° to 140° with an exposure of 30 min. The X-ray source operating mode was set to 25 kW/4 mA. A mineral phase analysis was performed with Match! 3 software (Crystal Impact, Bonn, Germany).

An Axios Max X-ray fluorescence (XRF) spectrometer (Panalytical, Almelo, The Netherlands) was used to analyse the solid residue after pulp filtration. The Fe (2+) content in the solid residue was determined using a chemical analysis (the dichromate titrimetric method was used for the total iron measurement, with the trivalent content being deduced after a full reduction using stannous chloride). Scanning electron microscopy with energy-dispersive X-ray spectroscopy (SEM-EDX, Vega III, Tescan, Brno, Czech Republic) was used to study the surface morphology and elemental composition of the solid residue.

2.4. Calculations

Using the setup in Figure 3a, the current density was calculated based on the active area of the current supply (stainless-steel plates). When the mesh was in contact with the solid (Figure 3b), there were particles that acted as a cathode surface themselves, creating a bulk cathode. It was, therefore, difficult to calculate the surface of the cathode, and only the current was estimated as a function of the cathode potential.

The faradaic current efficiency was estimated by measuring the cathode mass before and after the experiment, and the resulting pulp was filtered to separate the solid residue, which was then analysed for iron (2+) content. The results of the calculations of the change in the cathode mass and the amount of magnetite in the solid residue (no elemental iron was detected in this solid residue) were summed up to determine the total current efficiency, according to Equations (11) and (13).

The electrode reaction at the cathode to produce magnetite (Equation (11)):

$$3Fe_2O_3 + H_2O + 2e \rightarrow 2Fe_3O_4 + 2OH^- \quad (11)$$

The electrochemical equivalent to produce magnetite was equal to (Equation (12)):

$$a_{Fe_3O_4} = \frac{M_{Fe_3O_4}}{96485} = 0.024 \mathrm{gC}^{-1}, \quad (12)$$

where $a_{Fe_3O_4}$—electrochemical equivalent of producing 1 g of magnetite, g C^{-1}; $M_{Fe_3O_4}$—magnetite molar mass, g mol^{-1}; 96,485—Faraday constant, C mol^{-1}. The electrode reaction at the cathode to produce iron (Equation (13)):

$$Fe_2O_3 + 3H_2O + 6e \rightarrow 2Fe + 6OH^- \quad (13)$$

The electrochemical equivalent to produce 1 g of iron was equal to (Equation (14)):

$$a_{Fe} = \frac{\mathrm{M}_{Fe}}{3 \cdot 96485} = 0.00019 \mathrm{gC}^{-1}, \quad (14)$$

where a_{Fe}—electrochemical equivalent of producing 1 g of iron, g C^{-1}; M_{Fe}—the molar mass of iron, g mol^{-1}. It took 12.4 times more electricity to produce a unit mass of iron than to produce a unit mass of magnetite.

When using the bulk cathode (Figure 3b), most reduction products were found in the solid residue. The current efficiency could be determined by knowing the amount of magnetite and iron in the solid residue, which, in practice, is often a challenging task or can be estimated using semiquantitative methods via XRD or Mössbauer spectroscopy [20]. Hence, the determination of the coefficient of current efficiency, rather than the faradaic current efficiency, was obtained by utilizing the bulk cathode.

In order to evaluate the coefficient of current efficiency by utilizing the bulk cathode, the pulp obtained was subjected to Bayer leaching in an aluminate solution at a temperature of 250 °C for a duration of 30 min, with a ratio of L:S (liquid-to-solid) equal to 3.5 to 1. This process resulted in the conversion of elemental iron into magnetite [29]. Since magnetite was obtained after the high-pressure oxidation of iron (Equations (15)–(17)), it was possible to calculate the electrolysis efficiency coefficient, which would take into account the share of current that was used to obtain magnetite both directly as a result of electrolysis and due to the chemical reactions of the obtained elemental iron in the high-pressure reactor.

$$Fe + H_2O + OH^- = HFeO_2^- + H_2, \quad (15)$$

$$Fe_2O_3 + HFeO_2^- = Fe_3O_4 + OH^-, \quad (16)$$

$$3Fe_2O_3 + H_2 = 2Fe_3O_4 + H_2O. \quad (17)$$

According to the stoichiometry of Equations (15)–(17), for one mole of Fe, three moles of magnetite or 12.4 g of magnetite per 1 g of iron were formed, which coincided with the ratio of electrochemical equivalents (Equations (12) and (14)). From experimental data [29], it was known that the presence of 8.33% Fe to the mass of hematite in the pulp allowed for the reduction of 60% hematite, i.e., 1 g of iron allowed the obtainment of 7.8 g of magnetite. The coefficient of the efficiency of current consumption for obtaining magnetite directly through electrolysis was 1.6 times greater than for obtaining iron with subsequent high-pressure leaching to form magnetite.

The efficiency coefficient was lower than the actual faradaic current efficiency, as per Equations (11)–(13), as it took into account the chemical transformation of the primary product of electrolysis, namely, metallic iron, into magnetite. The results of iron (2+) determination in the solid residue of Bayer leaching and the change in mass of the current-supplying mesh were used to determine the total effectiveness of the current consumption when employing the bulk cathode.

3. Results and Discussion

3.1. Voltametric Measurements during Electroreduction of Iron Minerals in Suspension of Raw Bauxite in Alkaline Solutions

The reduction efficiency of hematite in a suspension obtained by mixing BR from the MYTILINEOS Aluminium of Greece with 50% NaOH (591.1 g L^{-1} Na_2O) solution [24] was strongly dependent on the process temperature and the concentration of the solid. The present study used the Bayer process solution, in which bauxite was subsequently leached for alumina extraction, and an alkaline solution with a concentration of 400 g L^{-1} Na_2O to carry out similar investigations. Figure 4 shows the results of the voltametric measurements using a solution containing 150 g L^{-1} Al_2O_3 and 300 g L^{-1} Na_2O (Bayer process aluminate solution).

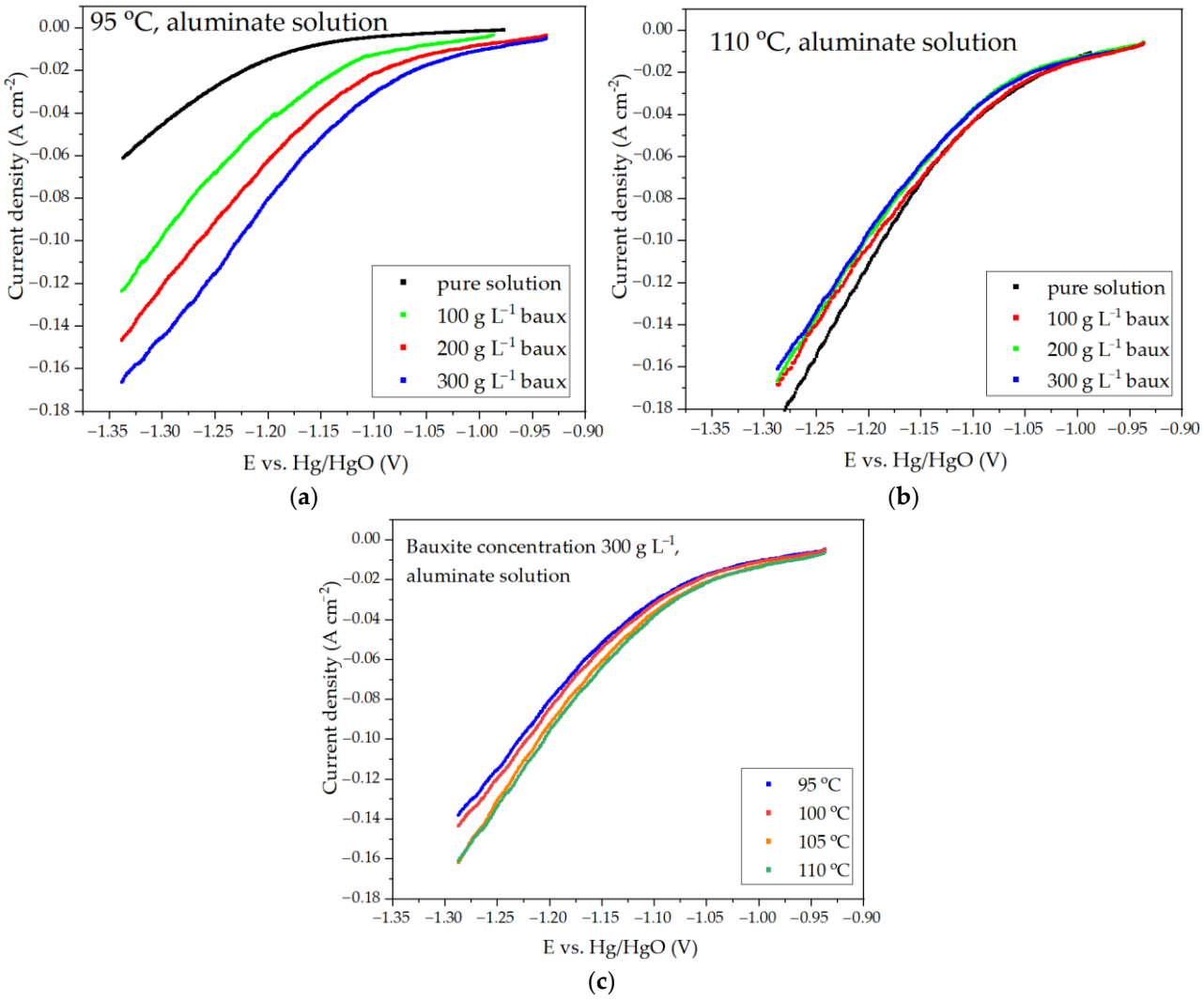


Figure 4. Dependence of current density on potential during electroreduction of iron minerals in suspension of bauxite in aluminate solution of Bayer process: (**a**) at different concentrations of solid at 95 °C; (**b**) at different concentrations of solid at 110 °C; (**c**) at different temperatures at solid concentration of 300 g L^{-1}.

As the aluminate solution used in the Bayer process contained only 300 g L^{-1} of caustic alkali, its boiling point was lower than that observed in studies using a solution with a concentration of 591 g L^{-1} Na_2O [24]. Therefore, the maximum temperature to which the solution was heated at atmospheric pressure in our experiments was 110 °C. The course of the voltametric curves shown in Figure 4a,b was significantly altered by increasing the amount of solid. Based on the data presented in Figure 4c, it could be observed that the overvoltage at the cathode decreased with the increasing temperature. If the rate of hematite reduction with the rise in cathodic potential was faster than the rate of hydrogen evolution, it could result in a decrease in the current share of the side reaction of hydrogen evolution and, consequently, an increase in the present efficiency.

As the temperature increased, a gradual convergence of the curves at various concentrations of solid in the suspension was observed. At 110 °C, the current density for a concentration of 300 g L^{-1} was even lower than for 100 and 200 g L^{-1}. This may have been due to a decrease in the concentration and kinetic limitations for hematite reduction, as well as a decrease in the overvoltage during hydrogen release. The true cause could be found by looking at how the current efficiency changed under different electrolysis conditions.

Further, the electrolysis was carried out for 2 h at different temperatures and solid concentrations (similar to the conditions of the voltametric curves in Figure 4) under potentiostatic conditions at a potential of −1.15 V, which, according to the literature data, corresponded to the beginning of the reduction of hematite and magnetite to elemental iron [25,30]. The results of determining the current efficiency of electrolysis are shown in Figure 5.

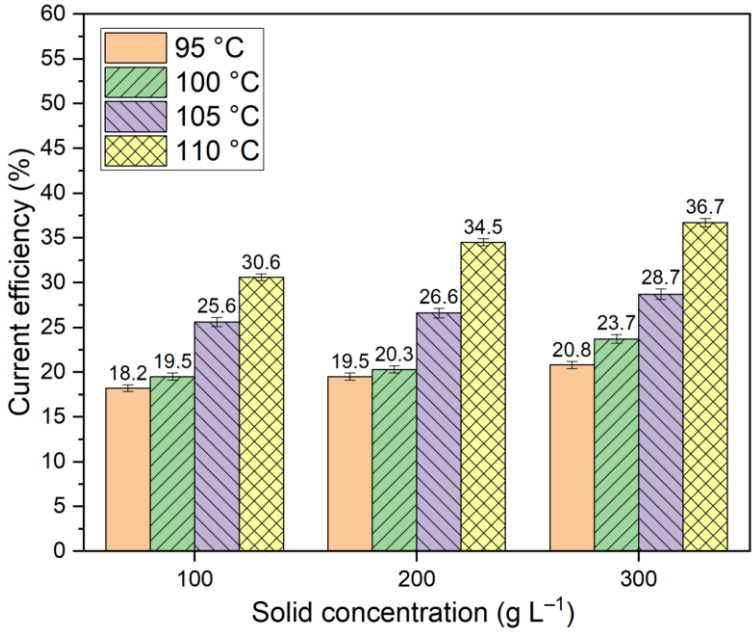


Figure 5. Results of current efficiency calculations at different temperatures and solid concentrations during the reduction of iron minerals for 2 h using a suspension of bauxite in aluminate Bayer solution.

The data presented in Figure 5 indicated that as the temperature rose, the proportion of current directed towards the reduction of iron minerals increased. The decrease in polarization with the increasing temperature and increasing concentration of solid in the suspension was due to the stronger influence of these factors on the rate of hematite and other iron-containing minerals reduction than their influence on the rates of side reactions.

At the same time, the current efficiency of the process of reducing hematite with a suspension of bauxite in an aluminate solution was inefficient because most of the current was still used to release hydrogen. In the process of reducing iron minerals with a suspension in an aluminate solution, all the iron was deposited at the cathode and the amount of magnetite or iron in the solid residue was small. The investigation of the morphology of the solid precipitate on the cathode is shown in Section 3.3.

According to the literature data, the electroreduction of hematite involves the transfer of iron into solution and the formation of $Fe(OH)_4^-$ complexes, which are then reacted at the cathode to produce dendritic iron [22]. There is a possibility of the formation of $Fe(OH)_3^-$ complexes, which, in turn, interact with hematite to form magnetite (Equation (5)). When using the aluminate solution of the Bayer process, the rate of dissolution of iron is very low. Otherwise, leaching in the refinery would produce solutions with a higher iron content, which, in practice, is not observed even with the use of high-pressure processes. This explains the low efficiency of the hematite electroreduction process using the aluminate solution, as well as the low amount of magnetite in the solid residue.

The studies were continued using an alkaline solution without dissolved alumina at a concentration of 400 g L^{-1} of Na_2O. According to our previous studies [27], this concentration is sufficient for the formation of magnetite from hematite in the presence of iron (2+) at temperatures above 110 °C, indicating the dissolution of hematite. Furthermore,

this concentration permits the suspension temperature to reach a temperature of 130 °C at atmospheric pressure [31]. The results of the cyclic voltametric (CV) measurements using a solution containing 400 g L^{-1} Na_2O at 120 °C are shown in Figure 6. To detect cathodic and anodic peaks, measurements were carried out at different scanning rates of 10 to 50 mV/s for 30 cycles.

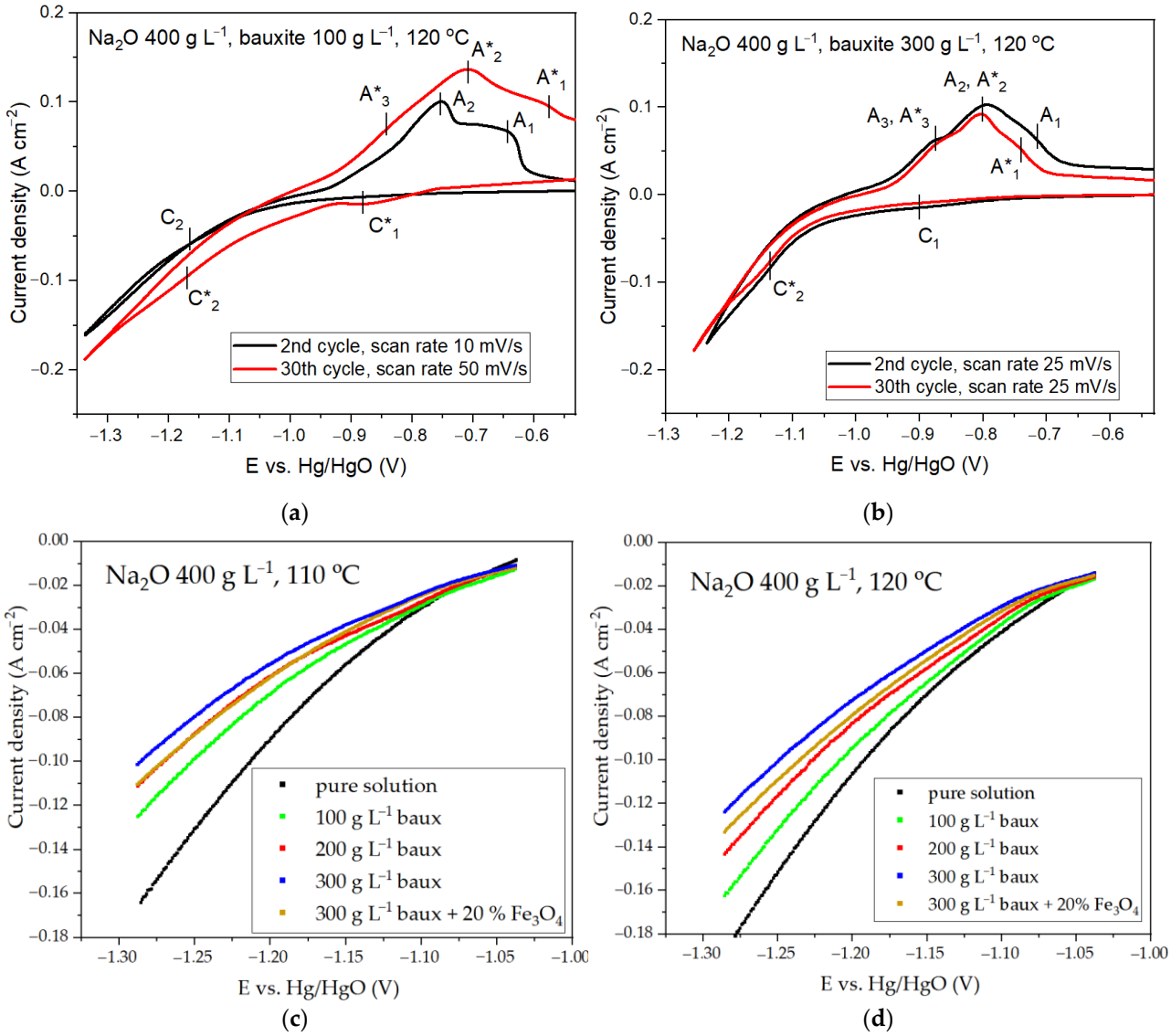


Figure 6. Dependence of current density on potential during electroreduction of bauxite iron minerals in alkaline solution with concentration of 400 g L^{-1}: (**a**) cyclic voltammetry (CV) at temperature 120 °C and solid concentration 100 g L^{-1}; (**b**) CV at temperature 120 °C and solid concentration 300 g L^{-1}; (**c**) potentiodynamic measurements at temperature 110 °C at different solid concentrations; (**d**) potentiodynamic measurements at temperature 120 °C at different solid concentrations.

According to Figure 6a,b, increasing the amount of solid in the suspension from 100 g L^{-1} to 300 g L^{-1} led to significant depolarization and an increase in the current density under otherwise equal conditions. This could indicate an increase in the rate of both the main and side reactions due to a decrease in the required overvoltage for the reaction to proceed. Figure 6a,b show that there were several cathodic and anodic peaks on the CV curves. The current C_1 with a potential E of −0.88 V was detected at the highest scan rate after 30 cycles and with a low solid concentration. According to research [25], this current was caused by the formation of iron (2+) compounds. It could have been both the formation

of $Fe(OH)_2$ and the reduction of iron (3+) hydroxocomplexes, according to Equation (3). The current C_2 was difficult to distinguish at a solid concentration of 100 g L^{-1} in the suspension, but became more distinct after 30 cycles at a solid concentration of 300 g L^{-1} at E = −1.14 V. This current was attributed to the reduction of magnetite and hematite to Fe [30]. In the initial stages of scanning at a low scanning speed, the cathodic peaks were not visible because they were overlapped by the side reaction of hydrogen evolution, which became predominant at cathodic potentials greater than 1.15 V.

At all concentrations of solid in the suspension, the anodic peaks were more distinct, since the oxidation process was not accompanied by the release of hydrogen. Peaks A_1 and A_3 were only visible as shoulders, while peak A_2 was clearly distinguishable. According to Monteiro et al. [25], the A_1 peak observed at a potential higher than E = −0.75 V could be attributed to the oxidation of compounds formed at the cathodic potential in the current C_1 region. The A_3 peak refers to the oxidation of Fe to $Fe(OH)_2$, and the A_2 peak refers to the oxidation of Fe to Fe^{2+} and the simultaneous completion of the oxidation of compounds formed at the A_3 current.

The potentiodynamic curves in Figure 6c,d showed that, with increasing temperature, the current density significantly increased over the entire potential range at the cathode for the pure solution (without bauxite) and for electroreduction from suspensions, which also indicated a general increase in the rate of the process. However, increasing the concentration of the solid phase in the suspension led to a decrease in the current density, which could indicate a decrease in the rate of the side reaction of hydrogen evolution.

A higher content of magnetite in the precipitate was observed when using an alkaline solution, which may have been due to the faster formation (at an increased alkali concentration and high temperature) of $Fe(OH)_4^-$ complexes, which were then reduced at the cathode to produce $Fe(OH)_3^-$. The latter interacted with hematite to form magnetite. The artificial addition of magnetite to bauxite resulted in a slight increase in the current density at the same concentration of bauxite in the suspension, which could indicate an increase in the reduction rate. It is possible that adding electroconductive magnetite [18] would increase the area of contact between the hematite particles and the cathode through the mechanism shown in Figure 7. However, the addition of magnetite could increase the amount of the iron-containing solid phase in contact with the cathode, which could also have a positive effect on the current efficiency. Nonetheless, the current efficiency of the magnetite reduction in [18] was significantly lower than that of the hematite reduction. The low current efficiency of the magnetite reduction process, its intensive formation under specific conditions and its electrically conductive properties resulted in a considerable amount of complexity in the description of the process involved, necessitating further investigation.

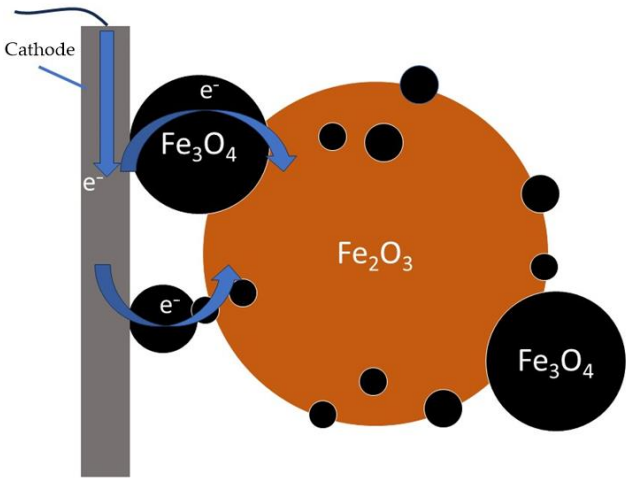


Figure 7. Mechanism of activating effect of magnetite.

In contrast to the electroreduction using an aluminate solution, the use of a relatively well dissolving hematite alkali solution led to a decrease in the current density at all temperatures relative to the pure solution (Figure 6), indicating an increase in the proportion of current going to the reduction of iron minerals in bauxite. Using an alkaline solution with a concentration of 400 g L^{-1} increased the total current efficiency at all concentrations and temperatures, as shown in Figure 8.

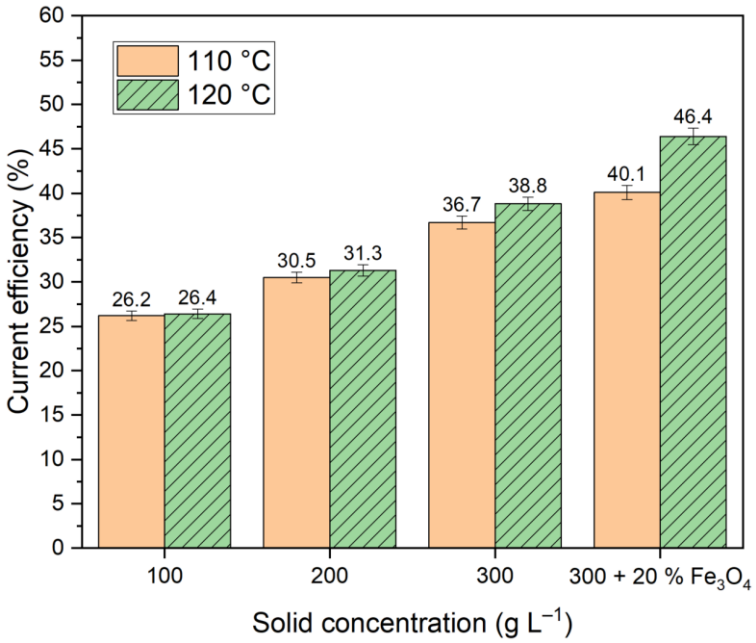


Figure 8. Results of current efficiency calculations at different temperatures and solid concentrations for iron mineral reduction for 2 h in suspension of bauxite in alkaline solution at a constant potential of −1.15 V.

It was evident that the addition of magnetite resulted in an enhancement of the current efficiency (Figure 8). Nevertheless, the obtained values of current efficiency were lower than those shown in studies [23,24], where the reduction of hematite from BR was carried out in a suspension of 50% NaOH solution. It could be associated with increased hydrogen evolution in our experiments due to the low concentration of the alkaline solution and the use of bauxite with a much lower iron content.

It is possible to conclude that, in order to increase the efficiency of the bauxite iron mineral reduction, it would be necessary to use an alkaline solution with a Na_2O concentration greater than 300 g L^{-1} to increase the concentration of bauxite in the suspension and to add magnetite to bauxite to maintain the cathodic potential below 1.15 V to reduce the share of current going to hydrogen release. The amount of solid in the suspension could be increased by using a thickening process and a bottom current supply that is in good contact with the entire volume of the solid phase, thereby creating a bulk cathode.

3.2. Electroreduction of Bauxite Iron Minerals Using Thickened Slurry and Mesh Current Supply (Bulk Cathode)

As demonstrated in the previous section, increasing the concentration of solids in the suspension could significantly increase the efficiency of the bauxite iron mineral reduction. In the subsequent experiments, a stainless-steel mesh current supply was utilized at the bottom of the beaker (Figure 3b). This supply was surrounded by bauxite particles during the thickening process, resulting in a significant increase in the quantity of solid in the cathode zone. The results of the voltametric measurements and electrolysis in the galvanostatic regime using a large mesh current supply (surface area 110 cm^2) are shown in Figure 9.

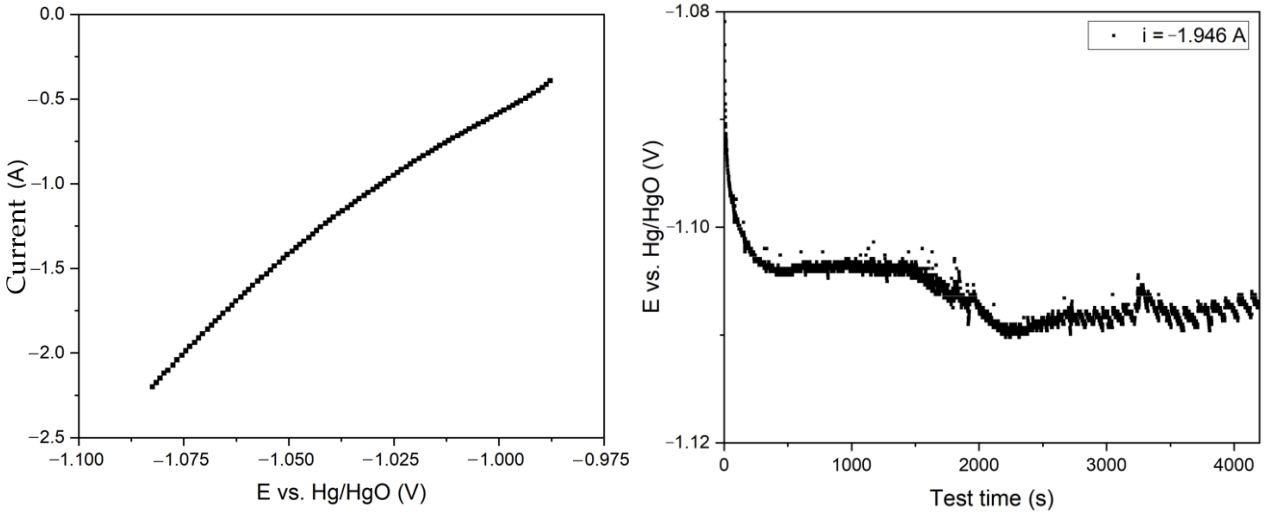


Figure 9. Results of experiments on electroreduction of bauxite iron minerals using a thickened slurry and a large mesh current supply with the surface area of 110 cm^2: (**a**) dependence of current on potential during electroreduction of bauxite minerals in alkali solution with the concentration of 400 g L^{-1}; (**b**) dependence of potential at the cathode on electrolysis time at a constant current of 1.945 A.

The figures in Figure 9 revealed that the cathode's potential was extremely low, corresponding to the initial almost straight line in Figure 6d. The current density in this section increased linearly with potential, and there was no visible hydrogen release, which began to progress at a high overvoltage.

At the beginning of the electrolysis process (Figure 9b), an increase in the potential from −1.080 V to −1.104 V was observed, followed by the establishment of a stable potential up to 1500 s (25 min), which allowed the process rate to be maintained at the same level. As the test duration increased, there was an increase in the overvoltage, which may be attributed to the completion of the reduction of particles contacting the current supply. A constant change in the suspension's colour to black was observed during the process, which may have been due to the beginning of magnetite reduction. The presence of magnetite on the surface of the particles caused it to be difficult to access the inner layers. This was due to the fact that the current efficiency for the conversion of pure magnetite to iron in the alkaline medium was rather low and strongly influenced by the porosity of the sample [25]. After 4200 s of electrolysis, the degree of conversion of Fe (3+) species to magnetite was 46.0%, which corresponded to a current efficiency coefficient of 60.7%. The yield of solid residue was 46.7%, which indicated an almost complete (>85%) dissolution of alumina after 1 h of desilication and subsequent electrolysis.

A series of experiments were conducted to investigate the effect of the duration of electrolysis with a large mesh current supply on the degree of Fe (3+) species and the current efficiency coefficient. In these experiments, all other conditions were the same, and the duration of electrolysis varied from 30 min to 210 min. Figure 10 shows the results of the experiments when changing the duration of electrolysis.

After 30 min of electrolysis, there was a noticeable decrease in the ratio of the reduction, and the current efficiency coefficient began to decrease. After 3.5 h, the maximum reduction ratio was 60.2%, but the current efficiency decreased from 81.4% after 30 min to 23.0% after 210 min of electrolysis. Thus, the process of iron mineral reduction was likely limited by diffusion through the magnetite layer formed on the surface of the reacting particles. The evidence supporting this conclusion was presented in the subsequent section. This explained the increase in the overvoltage observed after 25 min, as shown in Figure 9.

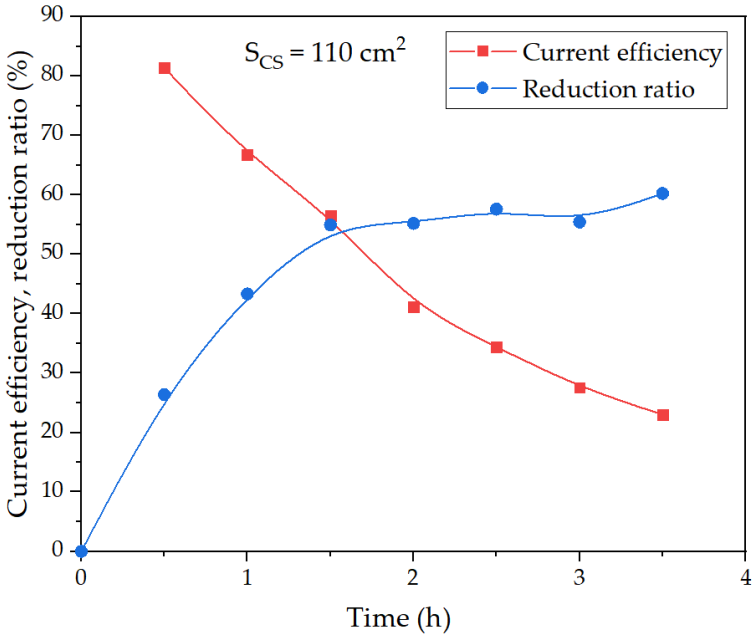


Figure 10. Effect of electrolysis duration using a large mesh current supply on the degree of iron (3+) species reduction and current efficiency coefficient at 100 g of bauxite per 300 cm^3 of alkaline suspension, temperature 120 °C and constant current 1.945 A.

The experiments were continued using a small mesh current supply (surface area 40 cm^2), with all other conditions being equal. The experimental results are shown in Figure 11.

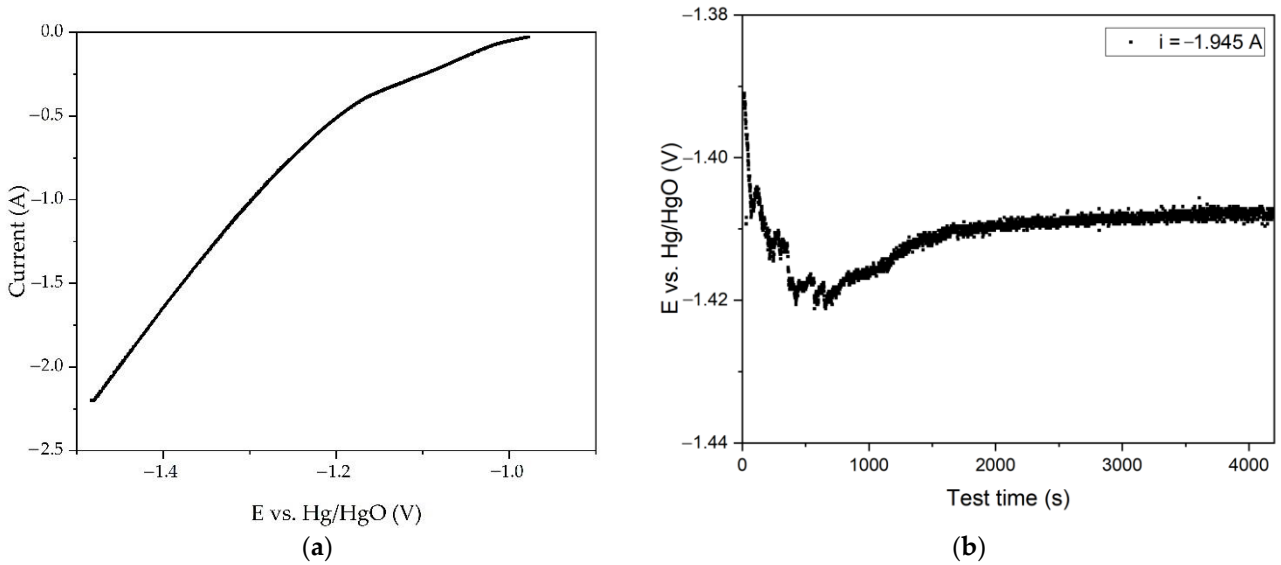


Figure 11. Results of experiments on electroreduction of bauxite iron minerals using a thickened pulp and a small mesh current supply with the area of 40 cm^2: (**a**) dependence of current on potential during electroreduction of bauxite minerals in alkali solution with the concentration of 400 g L^{-1}; (**b**) dependence of potential at the cathode on electrolysis time at a constant current of 1.945 A.

It was obvious that reducing the area of the current supply allowed for achieving a much higher potential (Figure 11a). The curve in this case had three sections: the first straight line, which reached a potential of −1.02 V, followed by a transient mode, where a current of −1.10 V, which corresponded to the current C_2 in Figure 6b, could be seen. It was, therefore, possible that this section was responsible for the reduction to metallic iron.

A sharp increase in the current began at a potential of −1.2 V, accompanied by a greater release of hydrogen.

The time dependence of the potential in the galvanostatic regime (i = 1.945 A), as depicted in Figure 11b, exhibited an inverse correlation in comparison to Figure 9b. At first, there was a slight increase in the potential, which could be explained by the deterioration of contact between the bauxite particles and the current supply with intense hydrogen evolution at a given current density. After 900 s of electrolysis, the potential at the cathode increased from an initial value of −1.390 V to −1.421 V. Then, a constant decrease in the potential to −1.410 V was observed. In these experiments, no severe darkening of the slurry due to magnetite formation was seen, and it was likely that a part of the iron minerals was converted to metallic iron. It was possible that the decrease in the overvoltage was due to the increase in the cathode area caused by iron forming on the surface of the current supply. The residue from electrolysis with a small surface area current supply was then leached at 250 °C for 30 min in a Bayer process aluminate solution. The degree of iron (3+) mineral deoxidation to magnetite was 38%. Therefore, the proportion of current used for the magnetite formation was less.

When studying the effect of the duration of electrolysis on the degree of reduction and current efficiency using a small current supply (Figure 12), a decrease in the efficiency of the process with time was observed, but a sharp decrease began not after 30 min, but after 1 h of electrolysis. The current efficiency coefficient was lower than when a larger area current supply was used.

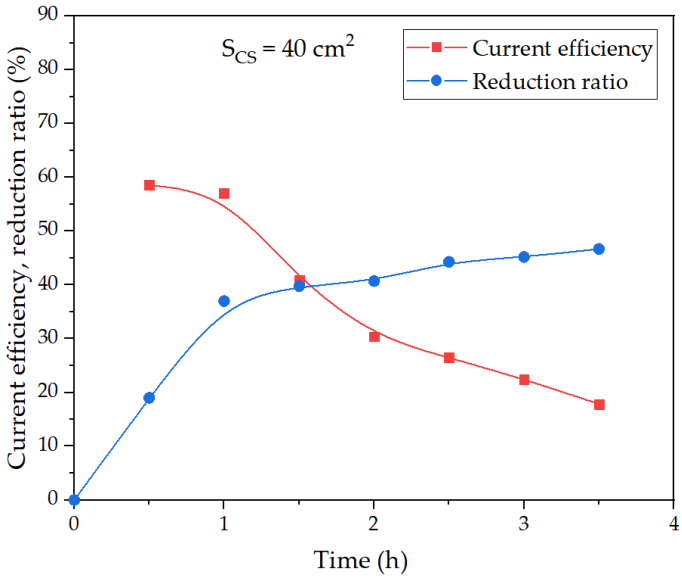


Figure 12. Effect of electrolysis duration using a small mesh current supply on the degree of iron (3+) species reduction and current efficiency coefficient at 100 g of bauxite per 300 cm^3 of alkaline suspension, temperature 120 °C and constant current 1.945 A.

The yield of solid residue using a current supply with a smaller area (experiment, the results of which are shown in Figure 11b) was 51.7%. After the leaching of this solid residue in the Bayer solution at 250 °C for 30 min, the yield of BR decreased to 34% (Al extraction was higher than 98%).

The high overvoltage led to a lower degree of reduction and, therefore, a low current efficiency coefficient (Figure 12), because the rate of the side reaction of hydrogen evolution increased. An attempt was carried out to conduct the experiment at a potential corresponding to the reduction of hematite into elemental iron (−1.15 V). When the overvoltage was not sufficient for an intensive hydrogen evolution. For this purpose, we experimentally selected a surface area of stainless-steel mesh where the potential at the cathode was −1.15 V during the potentiometric measurements at a current of 1.945 A. The

results of the experiments with a medium current supply (surface area 75 cm^2) are shown in Figure 13.

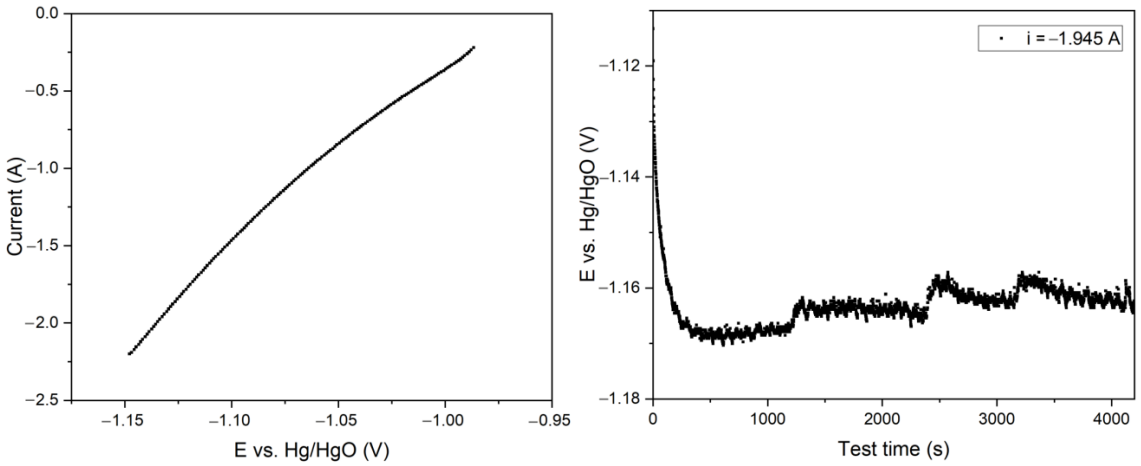


Figure 13. Results of experiments on electroreduction of bauxite iron minerals using a thickened pulp and a medium mesh current supply with the area of 75 cm^2: (**a**) dependence of current on potential during electroreduction of bauxite minerals in alkali solution with the concentration of 400 g L^{-1}; (**b**) dependence of potential at the cathode on electrolysis time at a constant current of 1.945 A.

The voltametric curve presented in Figure 13a and obtained using a medium-sized current supply was similar to the curve in Figure 9. However, in contrast to the electrolysis with a large area current supply at a current of 1.945 A, the potential at the cathode was −1.15 V, which favoured the production of the metallic iron. In fact, Figure 13b shows that after 1 h of electrolysis, the overvoltage at the cathode decreased. This was because metallic iron formed on the surface of the cathode, thereby increasing the surface of the current supply.

Figure 14 shows the dependence of the current efficiency coefficient and the degree of bauxite iron mineral reduction using a medium-sized current supply (the average value of the potential at the cathode in these experiments was −1.16 V) on the duration of electrolysis.

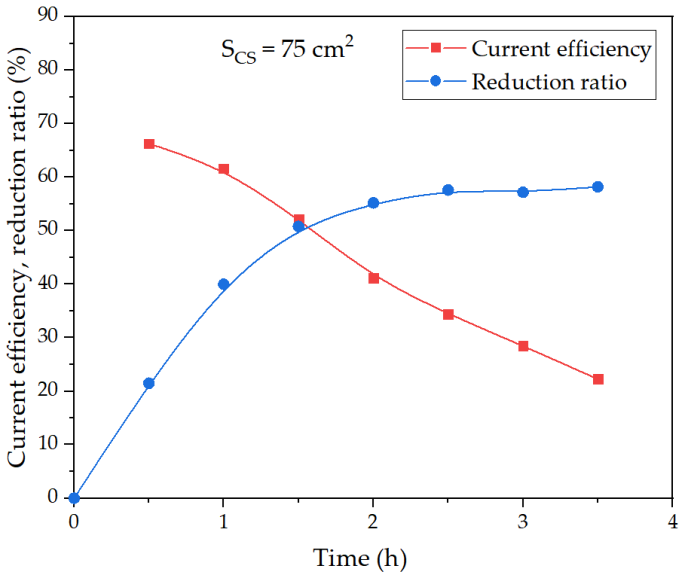


Figure 14. Effect of electrolysis duration using a medium mesh current supply on the degree of iron (3+) species reduction and current efficiency coefficient at 100 g of bauxite per 300 cm^3 of alkaline suspension, temperature 120 °C and constant current 1.945 A.

It was obvious that at an average potential at the cathode of −1.16 V, the results obtained were intermediate between large and small area current supplies. After 30 min of electrolysis, the current efficiency coefficient amounted to 66%, and after an hour, it decreased only by 5%. The current efficiency coefficient dropped more significantly than at the current supply with a surface area of 40 cm^2. After 3.5 h of electrolysis, the reduction ratio of bauxite iron minerals reached 58%, which was only 2% lower than at a larger area current supply.

Thus, the use of a bulk cathode and an alkaline solution with a concentration of 400 g L^{-1} Na_2O allowed for a significant increase in the current efficiency (>70%) if the target reduction ratio of bauxite iron minerals did not exceed 50%.

3.3. Solid Product Characterization

Figure 15 shows a SEM image of the precipitate that formed on the cathode's surface during electrolysis with a cathode immersed in a suspension of bauxite in the aluminate solution at 110 °C and a current density of 0.06 A cm^{-2}. The observed phenomenon indicated that, at low current densities, spherical-shaped precipitates were formed during electrolysis in the Bayer process solution. The spherical shape of the precipitate indicated a low iron content in the solution. Under these conditions, the solubility of hematite in the alkaline solution did not exceed 2×10^{-3} mol L^{-1} [25].

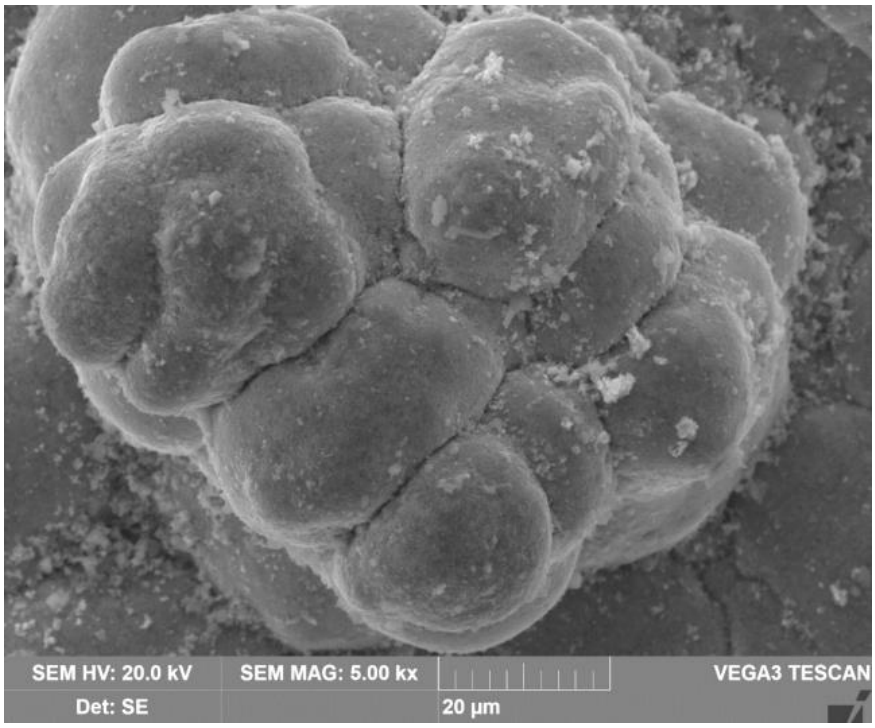


Figure 15. SEM image of the precipitate on the surface of the cathode during electrolysis in a suspension of bauxite in aluminate solution at 110 °C and a current density of 0.06 A cm^{-2}.

Figure 16 shows the distribution of elements on the cathode precipitate's surface. It was evident that the particles present on the cathode surface predominantly comprised iron and minor impurities of aluminium and silicon, which may be attributed to the physical inclusion of the suspension during metal deposition. The XRD pattern of the precipitate shown in Figure 17 confirmed the presence of α-iron as the main phase.

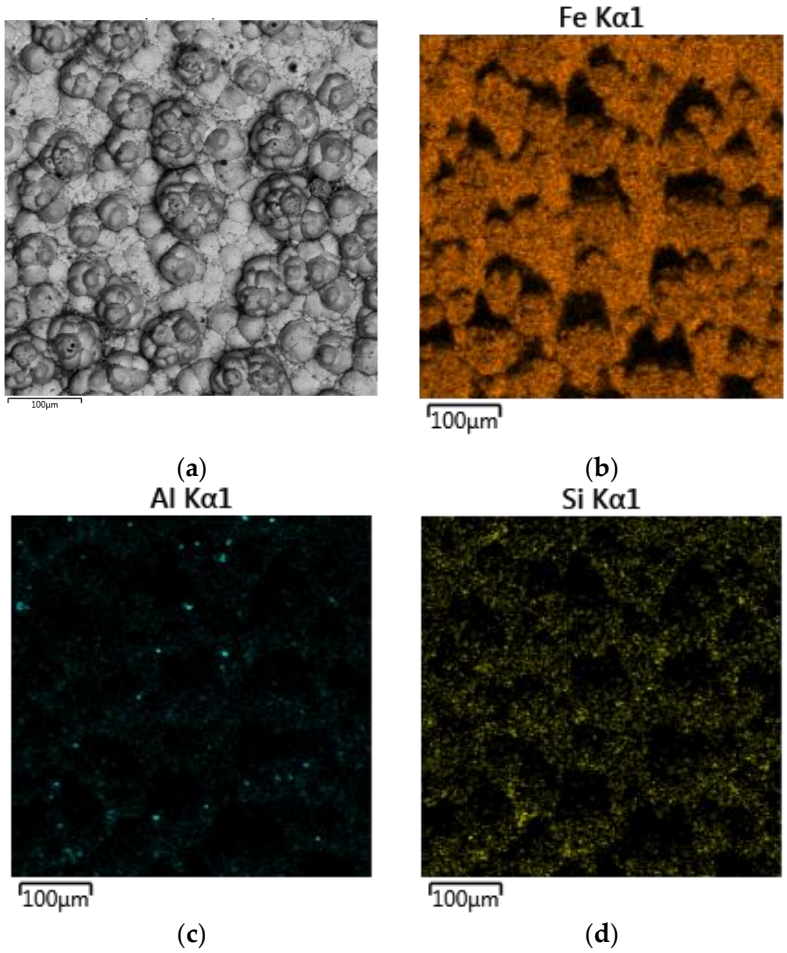


Figure 16. Maps of the distribution of elements on the surface of the cathode precipitate formed during electrolysis in a suspension of bauxite in aluminate solution at 110 °C and a current density of 0.06 A cm^{-2}: (**a**) SEM image of particle surface; (**b**) Fe distribution map; (**c**) Al distribution map; (**d**) Si distribution map.

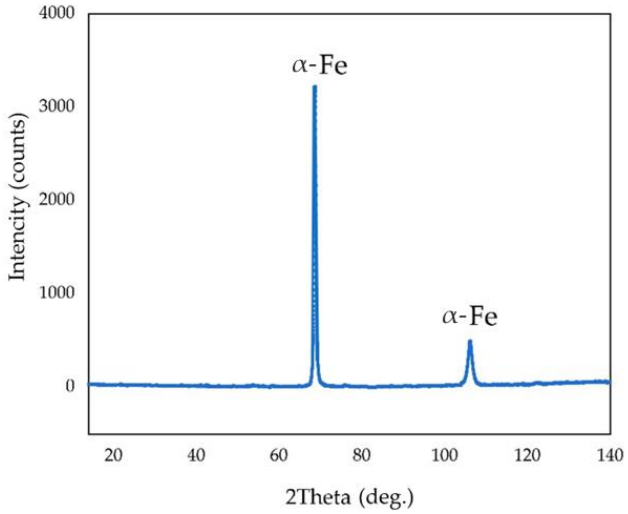


Figure 17. XRD pattern of the cathode precipitate formed during electrolysis in a suspension of bauxite in aluminate solution at 110 °C and a current density of 0.06 A cm^{-2}.

Figure 18 shows the results of the SEM-EDS analysis of the solid residue obtained using a large mesh current supply during 1.17 h of electrolysis. It could be seen that the

solid residue consisted of individual particles of aluminium and iron-containing phases. The results of the chemical composition of this solid residue indicated that Si was associated with Al, which could indicate the formation of a desilication product. This was confirmed with the results of the chemical composition of the solid residue (Table 3). A particle with a higher iron content could also be seen in the SEM-images. Figure 19a shows this particle at a high magnification. Other particles with a high iron content were also found (Figure 19b).

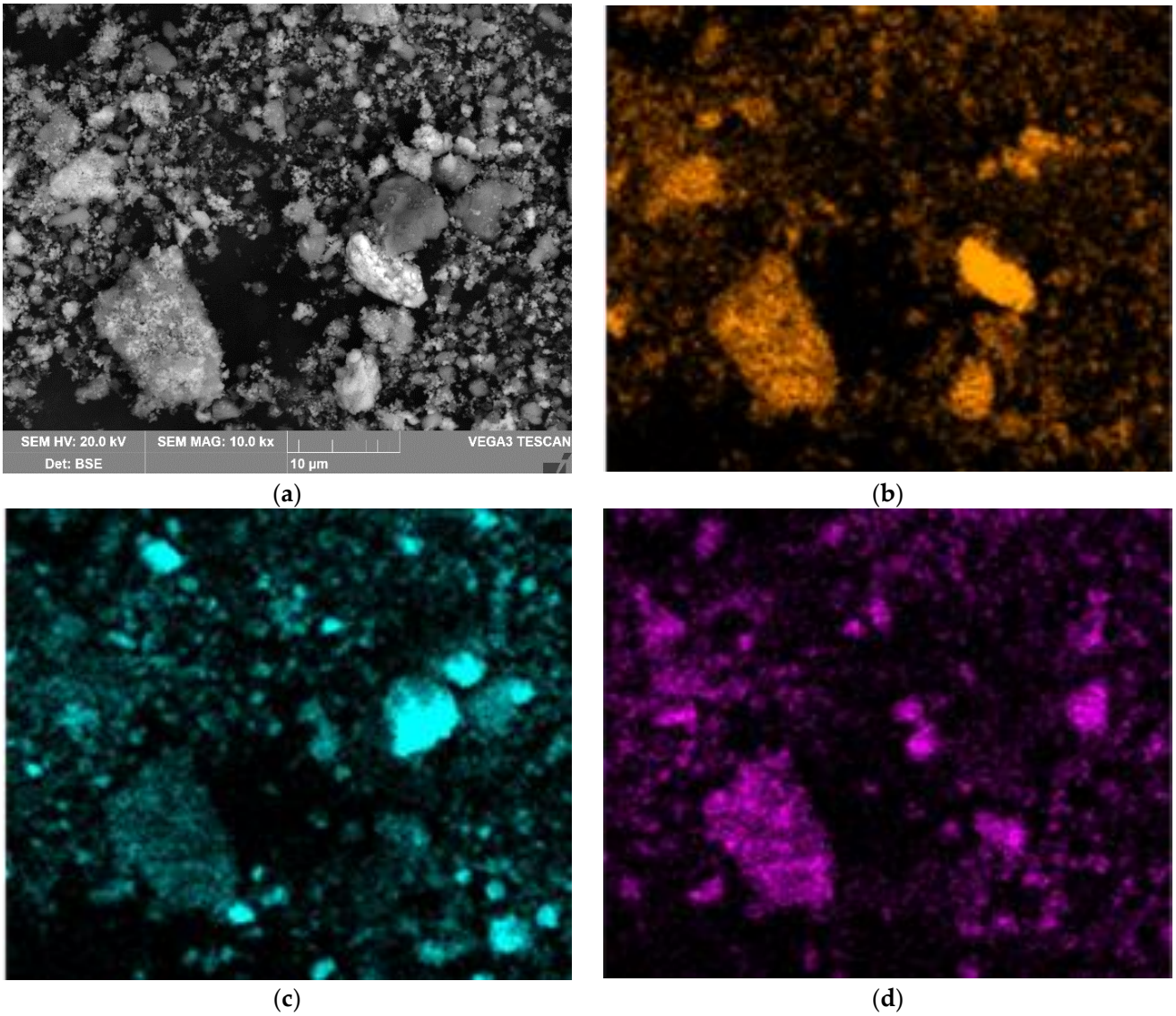
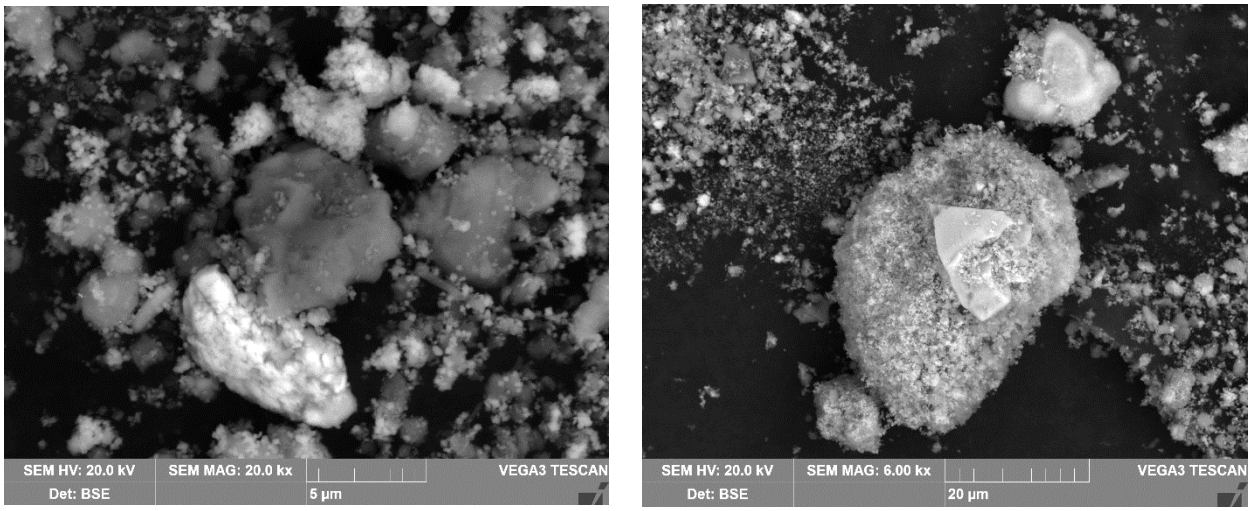


Figure 18. Results of SEM-EDS analysis of the surface of BR particles obtained after electrolysis with a large current supply for 1.17 h: (**a**) SEM image of particle surface; (**b**) Fe distribution map on the surface of particles in Figure 18a; (**c**) Al distribution map on the surface of particles in Figure 18a; (**d**) Si distribution map on the surface of particles in Figure 18a.

Table 3. Elemental composition of BR obtained after electrolysis with a large mesh current supply for 1.17 h, wt. %.

TFe *	Fe (2+)	Al	Si	Ti	Ca	Mn	Mg	Na	K	O
42.13	6.37	8.07	2.53	2.46	1.29	0.74	0.76	1.62	0.003	39.88

* TFe—total iron content.



(**a**) (**b**)

Figure 19. SEM images of BR particles with elevated iron content obtained after electrolysis with a large mesh current supply for 1.17 h: at magnitude ×20,000 (**a**), at magnitude ×6000 (**b**).

According to the SEM-EDS spectra, the mass percentage of iron on the surface of these particles was 75–80%, which was higher than the stoichiometric value for pure magnetite. This could indicate the presence of iron. Figure 20d shows the XRD diffraction pattern of the BR. It was evident that this BR was mainly composed of hematite and magnetite, with a small amount of unleached boehmite and the resulting desilication product.

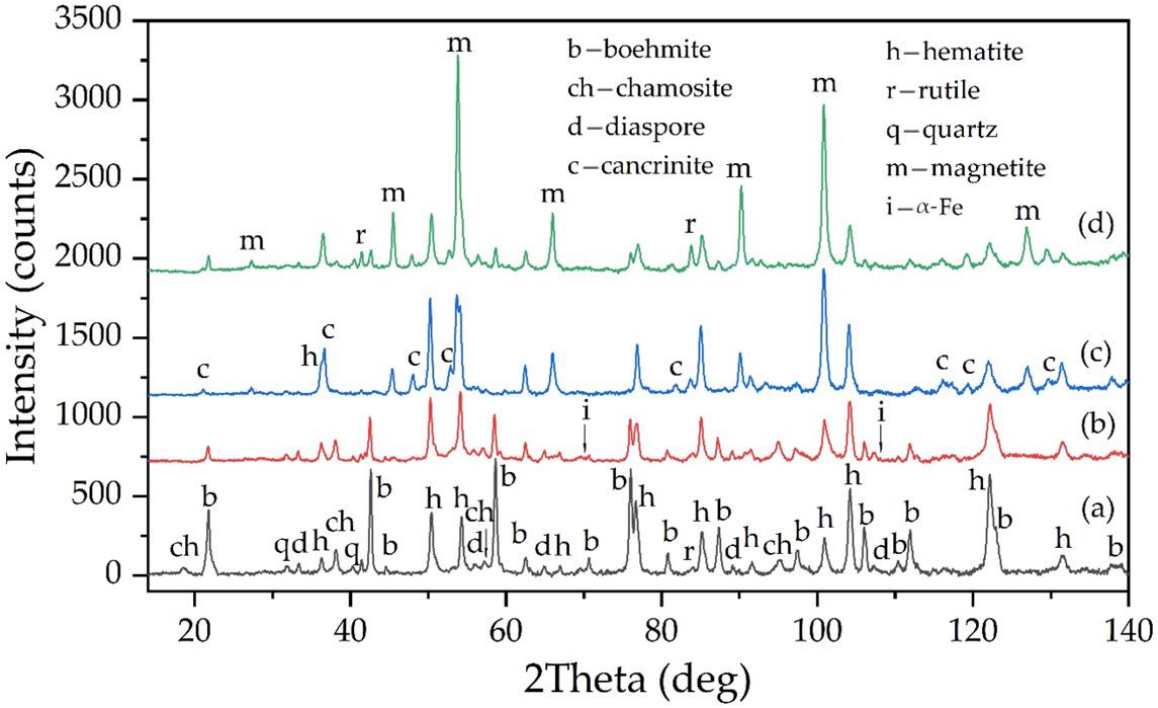


Figure 20. XRD pattern of: (**a**) raw bauxite; (**b**) solid residue obtained after electrolysis with a bulk cathode for 1.17 h at an average potential of −1.41 V; (**c**) BR obtained after leaching of solid residue from electrolysis with a bulk cathode and a potential of −1.41 V; (**d**) red mud obtained after electrolysis with a bulk cathode for 1.17 h at an average potential of −1.07 V.

The results of the SEM-EDS analysis of the solid residue obtained using a large mesh current supply during 1.17 h of electrolysis are shown in Figure 21. The dendritic

morphology of these particles suggested that they were most likely formed through the reduction of the iron hydroxocomplexes on the surface of the current supply (Equation (4)). The results of the XRD analysis of this sample (Figure 20b) further confirmed the presence of elemental iron, revealing small peaks of α-Fe. After electrolysis at −1.41 V using a small current supply, the amount of magnetite in the solid residue was lower than in experiments with a large current supply. However, it increased after the Bayer high-pressure leaching of the solid residue from electrolysis (Figure 20c). This suggested that elemental iron reacted with the alkaline solution with the formation of magnetite [15], according to Equations (15)–(17).

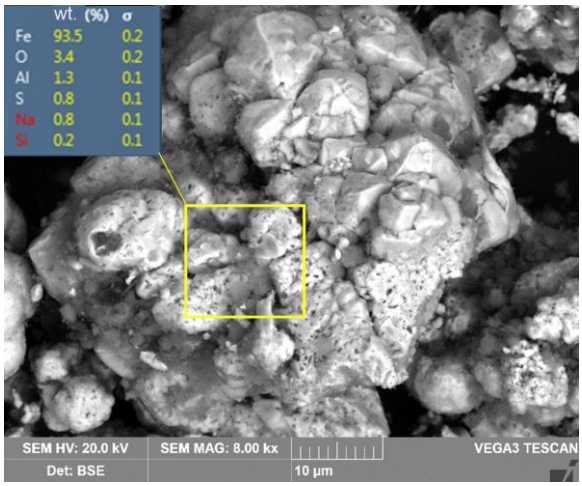


Figure 21. Microphotograph of elemental iron detected in the solid residue of electrolysis with a small current supply and the result of energy-dispersive analysis performed on the particle surface.

Table 4 shows the elemental composition of the solid residue after electrolysis with a small current supply for 1.17 h and the BR after two stages (electrolysis followed by leaching in Bayer solution at 250 °C for 30 min). The solid residue from electrolysis at the potential of the cathode −1.41 V had a higher concentration of alumina and a lower concentration of iron (2+), thereby confirming the incompleteness of the process of boehmite dissolution and iron mineral reduction. The formation of magnetite during the interaction of elemental iron with Bayer's solution resulted in a significant increase in the iron (2+) content after high-pressure leaching. Figure 22 shows SEM-EDS images of the BR after high-pressure leaching. The results of the SEM-EDS analysis of the BR showed that the iron was evenly distributed on the surface of the particles, and that aluminium and silicon were associated with Na in the form of a desilication product. There were also single independent particles of titanium compounds. Figure 23 shows the yield of the solid residue, the Al content in this solid residue and the Al extraction efficiency after electrolysis with a small and large mesh current supply. In Figure 23, the yield of the BR after the high-pressure leaching of the solid residue obtained after electrolysis with a small current supply is shown, as well as the Al content in this BR. The total Al extraction from bauxite after two stages of leaching (reductive and Bayer) was also shown.

Table 4. Elemental composition of the solid residue obtained after electrolysis with a small mesh current supply for 1.17 h and of the BR after its leaching with aluminate solution at T = 250 °C, τ = 30 min, C_{Na2O} = 300 g L^{-1} and C_{Al2O3} = 150 g L^{-1}, wt. %.

Sample	TFe	Fe(2+)	Al	Si	Ti	Ca	Mn	Mg	Na	K	O
Solid residue of electrolysis	37.91	4.39	15.36	1.74	2.28	1.47	0.52	0.51	0.42	0.005	39.79
BR	57.65	8.47	1.33	1.12	3.72	1.06	0.70	0.63	0.46	0.003	33.33

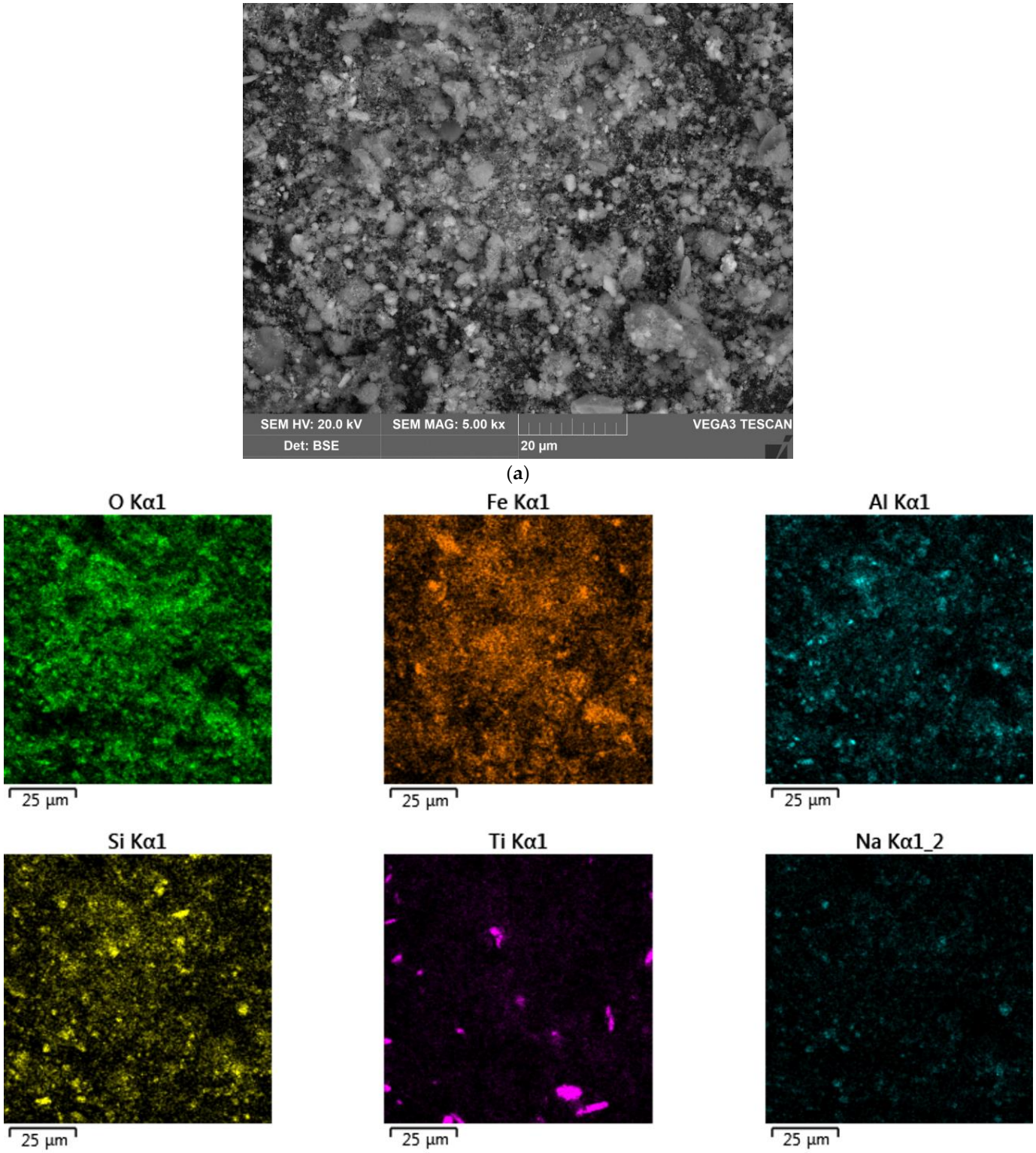


Figure 22. Results of SEM-EDS analysis of the surface of BR particles obtained after electrolysis with a small mesh current supply for 1.17 h and subsequent leaching with the Bayer process: (**a**) SEM image of the surface of BR particles; (**b**) map of elemental distribution on the particles' surface.

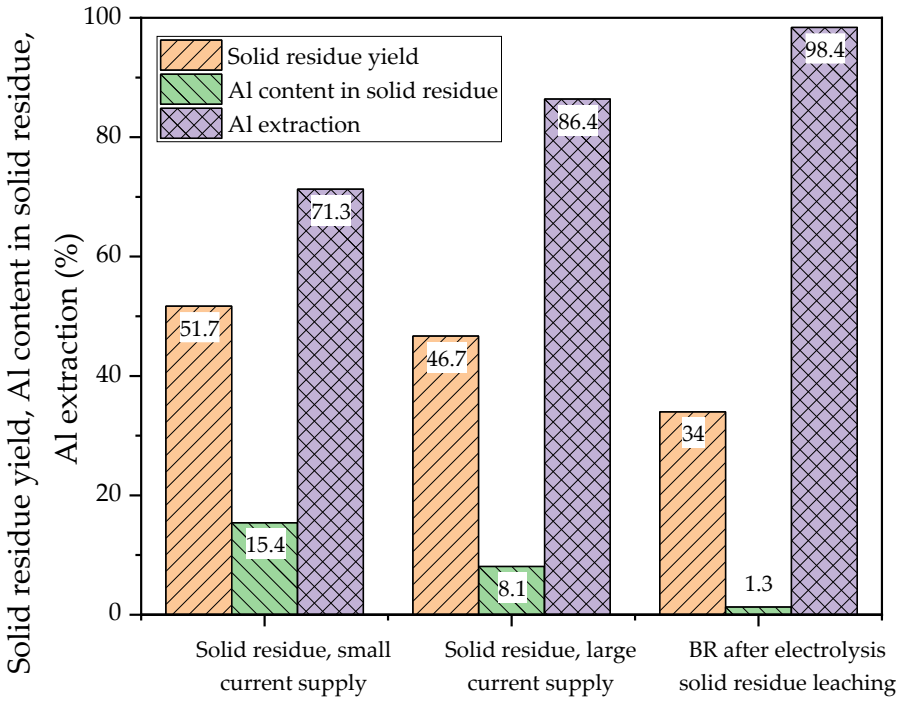


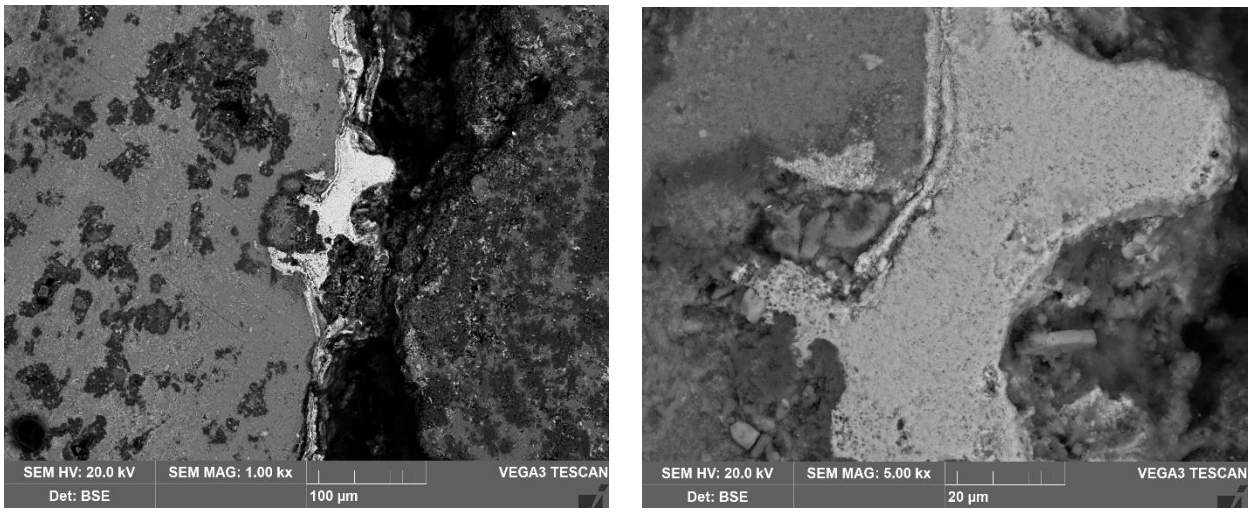
Figure 23. The yield of the solid residue, Al content in the solid residue and the Al extraction efficiency after electrolysis with a small and a large mesh current supply and after high-pressure leaching of electrolysis solid residue using Bayer aluminate solution.

A film of magnetite on the sample surface may have been responsible for the low degree of reduction (no more than 60% in Figure 10) and the attenuation of the process after 1 h of electrolysis. To confirm this, a SEM-EDS analysis of the surface of the solid residue coarse particle was performed (Figure 24).

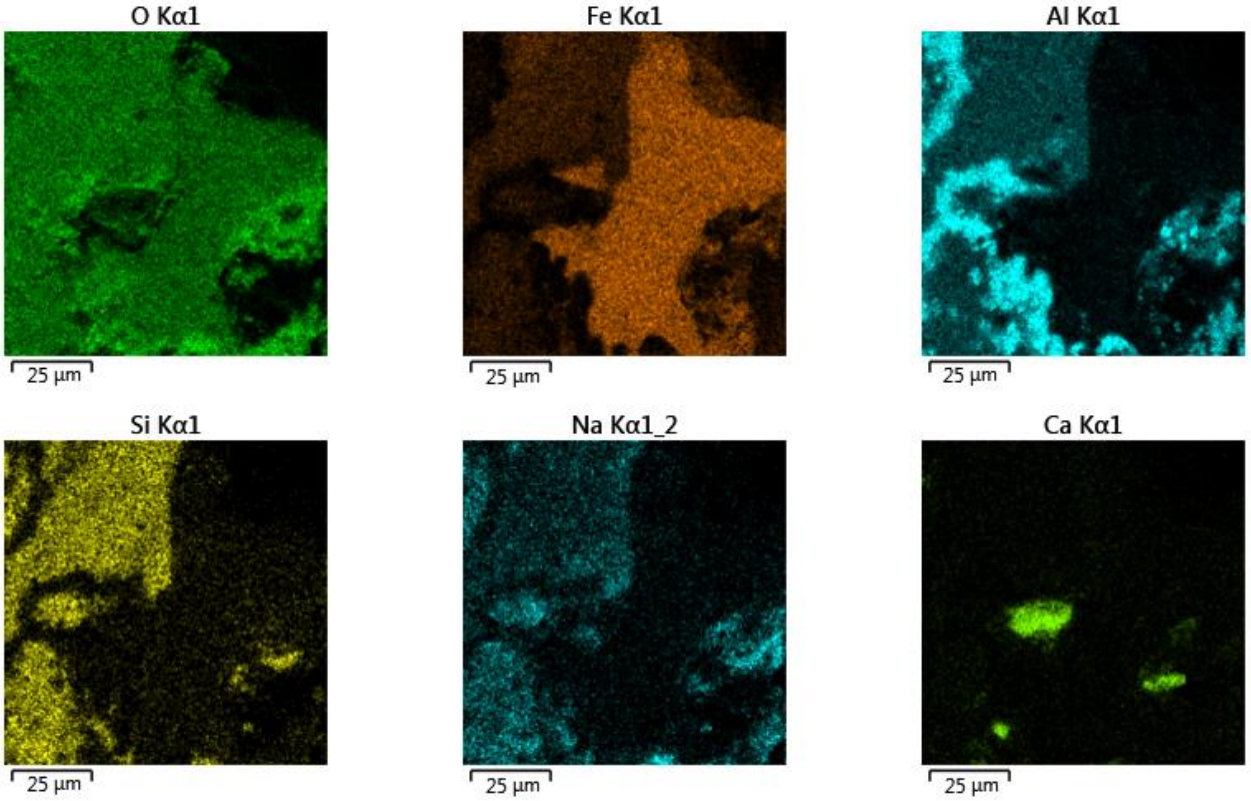
Figure 24a,b show a SEM image of one of the sections of the coarse particle revealing the formation of a solid film on the surface. As can be seen from Figure 24c, the phase with the increased iron content was found on the surface of the particle at the point of contact of the initial iron-bearing phase of bauxite with the solution. This suggested that the process proceeded mainly through dissolution. The presence of a lot of oxygen in all phases showed that magnetite was in the process of forming on the surface of the sample, not elemental iron.

Due to the dense layer of magnetite formed on the surface of the particle, it was impossible for the alkaline solution to penetrate further, thus, creating diffusion limitations. Additionally, the phase, which was in contact with the magnetite inside the particle, may not have had iron in its composition and be a dielectric, slowing down the process. To intensify the process, it was necessary to finely grind the raw material or to create conditions that favoured the complete dissolution of the iron-free phases, such as the preliminary desilication of the bauxite.

The results showed that, under the conditions of the experiments presented in this article, when using bauxite instead of pure hematite for reduction, two processes predominated: (1) the reduction of dissolved iron on the cathode surface; (2) the interaction of the iron-containing phase of bauxite with iron (2+) ions to form magnetite. Due to this, magnetite and elemental iron could be formed. The predominance of one or another product depended on the conditions of the process (temperature and concentration), the potential at the cathode, the method of current supply, etc.



(**a**) (**b**)



(**c**)

Figure 24. Results of SEM-EDS analysis of the surface of coarse BR particle obtained after electrolysis with a large mesh current supply: (**a**) SEM image of the surface of BR particle at magnitude ×1000; (**b**) SEM image of the surface of BR particle at magnitude ×5000; (**c**) map of element distribution on the particle surface.

The possibility of obtaining different products opens up several directions for further research, depending on the task. If it is necessary to reduce all hematite and other iron minerals in bauxite or BR to obtain a highly profitable product, a process using a suspension and a plate cathode in highly concentrated alkaline solutions should be used.

The reduction of iron minerals in the bauxite immediately with the extraction of aluminium could be achieved by employing a bulk cathode configuration with low alkali concentrations, resulting in the preferential formation of magnetite. The possible flowsheet

for the bauxite treatment with a bulk cathode configuration is shown in Figure 25. The consumption of electricity for the conversion of 1 t of Fe(3+) to Fe(2+) at a current efficiency of 80% was approximately 1050 kWh [32]. As such, for a 100% iron mineral reduction to Fe_3O_4, it would be necessary to reduce only one-third of Fe(3+) to an oxidation state +2 and the content of Fe in bauxite 180 kg t^{-1}. Then, the power consumption for the 50% reduction of Fe(3+) in 1 t of bauxite would be 1050 × 0.180 × 0.5/3 = 31.5 kWh. With the introduction of reduction leaching, the Al extraction from bauxite could be increased by 10%, which would mean lower costs for raw materials and basic materials, making it possible to justify the cost of electricity. Furthermore, the yield of BR would be decreased to 340 kg per every t of bauxite, which would lead to a decrease in maintenance costs and environmental pollution [33].

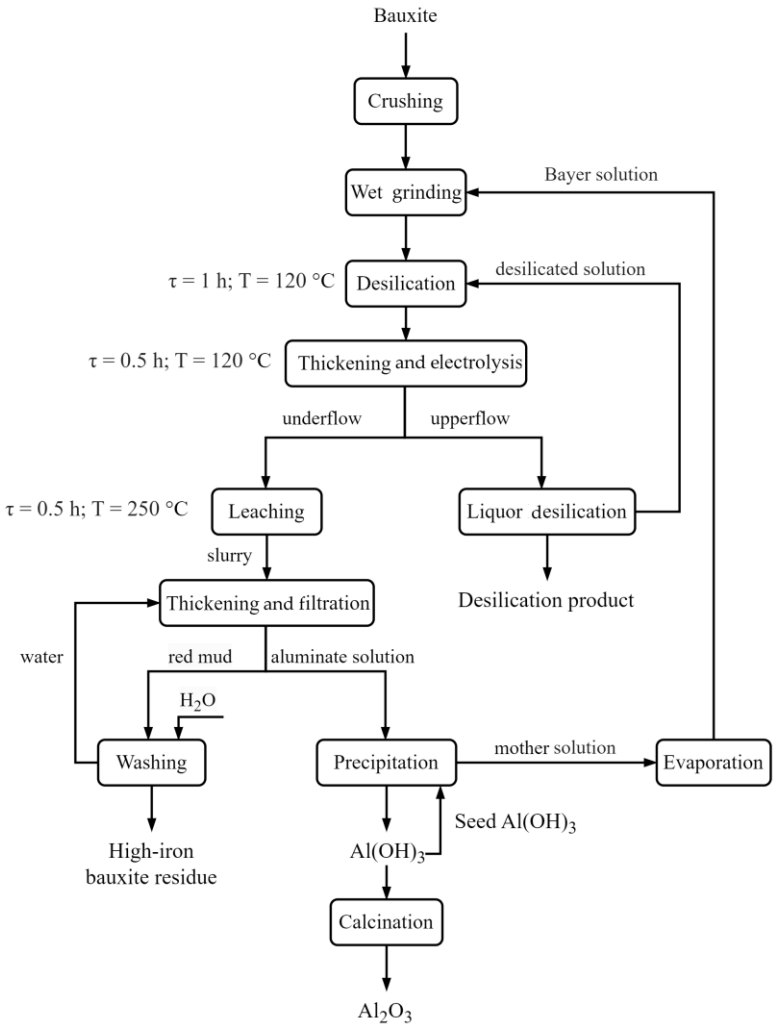


Figure 25. Flowsheet for the bauxite treatment using electroreductive Bayer process.

4. Conclusions

1. After the electrolytic reduction of bauxite iron minerals in a caustic alkali solution or aluminate solution, the following conclusions could be determined:
2. When using a cathode in the form of a plate immersed in a suspension of bauxite and aluminate solution of the Bayer process, the current efficiency did not exceed 30%, and the voltametric curve differed slightly from the pure solution, especially at temperatures below 100 °C, indicating the predominance of the side reaction of hydrogen formation.
3. The use of a suspension of bauxite in a caustic alkali solution with Na_2O concentration 400 g L^{-1} as a suspension with the concentration of solid being more than 300 g L^{-1}

allowed to increase the current efficiency due to a decrease in cathode polarization at elevated temperatures and a high amount of solid phase in the suspension. The addition of magnetite in the process of electrolysis allowed to increase the current efficiency at 120 °C up to 46%.

4. The experiment revealed that the application of the bulk cathode obtained through thickening the bauxite suspension on a stainless-steel mesh at the bottom of the reactor could significantly enhance the effectiveness of the electrolysis process at 120 °C. Within the first hour, it was possible to convert between 30 and 40% of Fe (3+) species to magnetite. The current efficiency coefficient under these conditions could reach 80%. As the duration of the process continued to increase, the current efficiency began to decrease.
5. The decrease in current efficiency with an increased electrolysis time may have been due to the passivation of the surface layer. The dense magnetite layer limited the advancement of the reaction front inside the particle, leading to a higher rate of side reactions.
6. It was shown that preliminary bauxite desilication and electrolytic reduction in a caustic alkali solution could produce a bauxite residue with more than 58% of total iron. Al extraction from bauxite could be increased to 98%.

Author Contributions: Conceptualization, A.S. and I.L.; methodology, A.S.; software, D.V.; validation, D.V. and I.L.; formal analysis, I.L.; investigation, A.S. and D.V.; resources, A.S.; data curation, A.S.; writing—original draft preparation, A.S. and D.V.; writing—review and editing, D.V. and I.L.; visualization, A.S.; supervision, A.S.; project administration, I.L.; funding acquisition, I.L. All authors have read and agreed to the published version of the manuscript.

Funding: This research was funded by RSCF, grant number 22-29-01515.

Data Availability Statement: All data were presented in this article.

Acknowledgments: The authors express their gratitude to Evgeny Kolesnikov from NUST MISiS for assistance in the SEM and XRD analyses of the solid samples.

Conflicts of Interest: The authors declare no conflict of interest.

References

1. Authier-Martin, M.; Forté, G.; Ostap, S.; See, J. The Mineralogy of Bauxite for Producing Smelter-Grade Alumina. *JOM* **2001**, *53*, 36–40. [CrossRef]
2. Anich, I.; Bagshaw, T.; Margolis, N.; Skillingberg, M. The Alumina Technology Roadmap. In *Essential Readings in Light Metals*; Donaldson, D., Raahauge, B.E., Eds.; Springer International Publishing: Cham, Switzerland, 2016; pp. 94–99. ISBN 978-3-319-48574-4.
3. Hind, A.R.; Bhargava, S.K.; Grocott, S.C. The Surface Chemistry of Bayer Process Solids: A Review. *Colloids Surf. A Physicochem. Eng. Asp.* **1999**, *146*, 359–374. [CrossRef]
4. Smith, P. The Processing of High Silica Bauxites—Review of Existing and Potential Processes. *Hydrometallurgy* **2009**, *98*, 162–176. [CrossRef]
5. Alkan, G.; Schier, C.; Gronen, L.; Stopic, S.; Friedrich, B. A Mineralogical Assessment on Residues after Acidic Leaching of Bauxite Residue (Red Mud) for Titanium Recovery. *Metals* **2017**, *7*, 458. [CrossRef]
6. Anawati, J.; Azimi, G. Recovery of Scandium from Canadian Bauxite Residue Utilizing Acid Baking Followed by Water Leaching. *Waste Manag.* **2019**, *95*, 549–559. [CrossRef]
7. Zhou, G.; Wang, Y.; Qi, T.; Zhou, Q.; Liu, G.; Peng, Z.; Li, X. Enhanced Conversion Mechanism of Al-Goethite in Gibbsitic Bauxite under Reductive Bayer Digestion Process. *Trans. Nonferrous Met. Soc. China* **2022**, *32*, 3077–3087. [CrossRef]
8. Zhou, G.; Wang, Y.; Qi, T.; Zhou, Q.; Liu, G.; Peng, Z.; Li, X. Comprehensive Utilization of Al-Goethite-Containing Red Mud Treated Through Low-Temperature Sodium Salt-Assisted Roasting–Water Leaching. *J. Sustain. Metall.* **2022**, *8*, 825–836. [CrossRef]
9. Zhou, X.; Liu, G.; Qi, T.; Zhao, J.; Peng, Z.; Wang, Y.; Shen, L. Increasing Iron Recovery from High-Iron Red Mud by Surface Magnetization. *J. Sustain. Metall.* **2023**, *9*, 795–805. [CrossRef]
10. Li, X.; Yu, S.; Dong, W.; Chen, Y.; Zhou, Q.; Qi, T.; Liu, G.; Peng, Z.; Jiang, Y. Investigating the Effect of Ferrous Ion on the Digestion of Diasporic Bauxite in the Bayer Process. *Hydrometallurgy* **2015**, *152*, 183–189. [CrossRef]
11. Wang, Y.; Li, X.; Zhou, Q.; Qi, T.; Liu, G.; Peng, Z.; Zhou, K. Effects of Si-Bearing Minerals on the Conversion of Hematite into Magnetite during Reductive Bayer Digestion. *Hydrometallurgy* **2019**, *189*, 105126. [CrossRef]

12. Wang, Y.; Li, X.; Wang, B.; Zhou, Q.; Qi, T.; Liu, G.; Peng, Z.; Zhou, K. Interactions of Iron and Titanium-Bearing Minerals under High-Temperature Bayer Digestion Conditions. *Hydrometallurgy* **2019**, *184*, 192–198. [CrossRef]
13. Pasechnik, L.A.; Skachkov, V.M.; Bogdanova, E.A.; Chufarov, A.Y.; Kellerman, D.G.; Medyankina, I.S.; Yatsenko, S.P. A Promising Process for Transformation of Hematite to Magnetite with Simultaneous Dissolution of Alumina from Red Mud in Alkaline Medium. *Hydrometallurgy* **2020**, *196*, 105438. [CrossRef]
14. Zhou, G.; Wang, Y.; Zhang, Y.; Qi, T.; Zhou, Q.; Liu, G.; Peng, Z.; Li, X. A Clean Two-Stage Bayer Process for Achieving near-Zero Waste Discharge from High-Iron Gibbsitic Bauxite. *J. Clean. Prod.* **2023**, *405*, 136991. [CrossRef]
15. Li, X.; Wang, Y.; Zhou, Q.; Qi, T.; Liu, G.; Peng, Z.; Wang, H. Transformation of Hematite in Diasporic Bauxite during Reductive Bayer Digestion and Recovery of Iron. *Trans. Nonferrous Met. Soc. China* **2017**, *27*, 2715–2726. [CrossRef]
16. Allanore, A.; Lavelaine, H.; Valentin, G.; Birat, J.P.; Lapicque, F. Electrodeposition of Metal Iron from Dissolved Species in Alkaline Media. *J. Electrochem. Soc.* **2007**, *154*, E187–E193. [CrossRef]
17. Ivanova, Y.A.; Monteiro, J.F.; Horovistiz, A.L.; Ivanou, D.K.; Mata, D.; Silva, R.F.; Frade, J.R. Electrochemical Deposition of Fe and Fe/CNTs Composites from Strongly Alkaline Hematite Suspensions. *J. Appl. Electrochem.* **2015**, *45*, 515–522. [CrossRef]
18. Feynerol, V.; Lavelaine, H.; Marlier, P.; Pons, M.-N.; Lapicque, F. Reactivity of Suspended Iron Oxide Particles in Low Temperature Alkaline Electrolysis. *J. Appl. Electrochem.* **2017**, *47*, 1339–1350. [CrossRef]
19. Allanore, A.; Lavelaine, H.; Valentin, G.; Birat, J.P.; Lapicque, F. Iron Metal Production by Bulk Electrolysis of Iron Ore Particles in Aqueous Media. *J. Electrochem. Soc.* **2008**, *155*, E125. [CrossRef]
20. Allanore, A.; Lavelaine, H.; Valentin, G.; Birat, J.P.; Delcroix, P.; Lapicque, F. Observation and Modeling of the Reduction of Hematite Particles to Metal in Alkaline Solution by Electrolysis. *Electrochim. Acta* **2010**, *55*, 4007–4013. [CrossRef]
21. Ivanova, Y.A.; Monteiro, J.F.; Teixeira, L.B.; Vitorino, N.; Kovalevsky, A.V.; Frade, J.R. Designed Porous Microstructures for Electrochemical Reduction of Bulk Hematite Ceramics. *Mater. Des.* **2017**, *122*, 307–314. [CrossRef]
22. Zou, X.; Gu, S.; Lu, X.; Xie, X.; Lu, C.; Zhou, Z.; Ding, W. Electroreduction of Iron(III) Oxide Pellets to Iron in Alkaline Media: A Typical Shrinking-Core Reaction Process. *Metall. Mater. Trans. B* **2015**, *46*, 1262–1274. [CrossRef]
23. Maihatchi, A.; Pons, M.-N.; Ricoux, Q.; Goettmann, F.; Lapicque, F. Electrolytic Iron Production from Alkaline Suspensions of Solid Oxides: Compared Cases of Hematite, Iron Ore and Iron-Rich Bayer Process Residues. *J. Electrochem. Sci. Eng.* **2020**, *10*, 95–102. [CrossRef]
24. Koutsoupa, S.; Koutalidi, S.; Bourbos, E.; Balomenos, E.; Panias, D. Electrolytic Iron Production from Alkaline Bauxite Residue Slurries at Low Temperatures: Carbon-Free Electrochemical Process for the Production of Metallic Iron. *Johns. Matthey Technol. Rev.* **2021**, *65*, 366–374. [CrossRef]
25. Monteiro, J.F.; Ivanova, Y.A.; Kovalevsky, A.V.; Ivanou, D.K.; Frade, J.R. Reduction of Magnetite to Metallic Iron in Strong Alkaline Medium. *Electrochim. Acta* **2016**, *193*, 284–292. [CrossRef]
26. Lopes, D.V.; Lisenkov, A.D.; Sergiienko, S.A.; Constantinescu, G.; Sarabando, A.; Quina, M.J.; Frade, J.R.; Kovalevsky, A.V. Alkaline Electrochemical Reduction of a Magnesium Ferrospinel into Metallic Iron for the Valorisation of Magnetite-Based Metallurgical Waste. *J. Electrochem. Soc.* **2021**, *168*, 073504. [CrossRef]
27. Shoppert, A.; Valeev, D.; Loginova, I.; Pankratov, D. Low-Temperature Treatment of Boehmitic Bauxite Using the Bayer Reductive Method with the Formation of High-Iron Magnetite Concentrate. *Materials* **2023**, *16*, 4678. [CrossRef]
28. Shoppert, A.; Valeev, D.; Diallo, M.M.; Loginova, I.; Beavogui, M.C.; Rakhmonov, A.; Ovchenkov, Y.; Pankratov, D. High-Iron Bauxite Residue (Red Mud) Valorization Using Hydrochemical Conversion of Goethite to Magnetite. *Materials* **2022**, *15*, 8423. [CrossRef]
29. Wang, Y.; Li, X.; Zhou, Q.; Wang, B.; Qi, T.; Liu, G.; Peng, Z.; Pi, J.; Zhao, Z.; Wang, M. Reduction of Red Mud Discharge by Reductive Bayer Digestion: A Comparative Study and Industrial Validation. *JOM* **2020**, *72*, 270–277. [CrossRef]
30. Lopes, D.V.; Ivanova, Y.A.; Kovalevsky, A.V.; Sarabando, A.R.; Frade, J.R.; Quina, M.J. Electrochemical Reduction of Hematite-Based Ceramics in Alkaline Medium: Challenges in Electrode Design. *Electrochim. Acta* **2019**, *327*, 135060. [CrossRef]
31. Shoppert, A.; Loginova, I.; Valeev, D. Kinetics Study of Al Extraction from Desilicated Coal Fly Ash by NaOH at Atmospheric Pressure. *Materials* **2021**, *14*, 7700. [CrossRef]
32. Allanore, A.; Lavelaine, H.; Birat, J.P.; Valentin, G.; Lapicque, F. Experimental Investigation of Cell Design for the Electrolysis of Iron Oxide Suspensions in Alkaline Electrolyte. *J. Appl. Electrochem.* **2010**, *40*, 1957–1966. [CrossRef]
33. Zeng, H.; Lyu, F.; Sun, W.; Zhang, H.; Wang, L.; Wang, Y. Progress on the Industrial Applications of Red Mud with a Focus on China. *Minerals* **2020**, *10*, 773. [CrossRef]

Disclaimer/Publisher's Note: The statements, opinions and data contained in all publications are solely those of the individual author(s) and contributor(s) and not of MDPI and/or the editor(s). MDPI and/or the editor(s) disclaim responsibility for any injury to people or property resulting from any ideas, methods, instructions or products referred to in the content.